Review of Heat Transfer Enhancement Techniques in Two-Phase Flows for Highly Efficient and Sustainable Cooling

Mohamed H. Mousa[1], Cheng-Min Yang[2], Kashif Nawaz[2*], Nenad Miljkovic[1,3,4,5*]

[1]*Department of Mechanical Science and Engineering, University of Illinois at Urbana – Champaign, 1206 W Green St, Urbana, Illinois 61801 USA*

[2]*Oak Ridge National Laboratory, Oak Ridge, TN, USA*

[3]*Department of Electrical and Computer Engineering, University of Illinois at Urbana – Champaign, 1206 W Green St, Urbana, Illinois 61801 USA*

[4]*Materials Research Laboratory, University of Illinois, Urbana, Illinois 61801, USA*

[5]*International Institute for Carbon Neutral Energy Research (WPI-I2CNER), Kyushu University, 744 Motooka, Nishi-ku, Fukuoka 819-0395, Japan*

Declarations of interest: none

* corresponding author details, nawazk@ornl.gov; nmiljkov@illinois.edu

ABSTRACT

Two-phase internal flow is ubiquitous to many systems due to its ability to transfer large amounts of heat effectively. Recent advances motivated by sustainability have pushed towards augmenting the heat transfer between the tube and the two-phase working fluid. Augmenting heat transfer in two-phase flows enables process intensification, and compactness leading to reduced cost and material consumption. This review investigates the effect of heat transfer enhancement techniques on different fluids including R134a, R407C, R22, etc... The techniques are categorized into passive and active and focus on durable enhancement methods which do not include surface structuring or coating. Passive techniques utilize geometrical and surface modifications to induce better mixing. Several passive techniques are analyzed including fins, inserts, and more. In analyzing these techniques, the effect of changing geometric parameters is studied, and the limitations are highlighted. Further, active techniques that enable heat transfer enhancement through applying power are also investigated. Electrohydrodynamic approaches are analyzed and compared to passive techniques. Additionally, the implications of heat exchange enhancement in the context of global energy are discussed. An energy analysis discretized by the use sector is conducted, with an emphasis on predicting the future potential for renewable and sustainable development. Moreover, although active approaches provide the highest heat transfer enhancement, due to implementation difficulties, passive techniques are more frequently adopted. The review ends with discussion of next-generation heat exchangers which will rely more on additive manufacturing due to its flexibility and reduced cost per part as the technology matures.

Highlights:

- Active methods provide heat transfer enhancement up to 20X
- Passive methods are cheaper compared to active but cause high pressure drop
- Passive methods disturb boundary layer development and maximize contact area
- Passive methods in flow boiling aim to maximize annular flow regimes
- Additive manufacturing is a key advancement in enhancement integration

Keywords: Boiling, Condensation, Augmentation, Swirl flow, Pressure drop, Passive, Active, Nusselt number, Friction factor, Additive manufacturing.

Word Count: 16834 words (excluding title, author names and affiliations, keywords, figure/table captions, abbreviations, acknowledgments, and references)

NOMENCLATURE

$\dot{m}$	mass flow rate (kg/s)
A	total inner surface area (m^2)
d	tube diameter (m)
C_p	specific heat capacity (kJ/kg·K)
e	depth of corrugated tube (m)
EF	enhancement factor (=$(hA)_{\text{Enhanced tube}}/(hA)_{\text{smooth tube}}$)
f	friction factor
G	mass flux (kg/(m^2·s))
h	convection heat transfer coefficient (W/(m^2·K))
h_{fg}	latent heat of vaporization (kJ/kg)
H	fin height (m)
k	thermal conductivity (W/(m·K))
L	length of test section (m)
$LMTD$	logarithmic mean temperature difference
Nu	Nusselt number (= hd/k)
p	helical pitch (m)
PF	pressure factor (= $(\Delta P)_{\text{Enhanced tube}}/(\Delta P)_{\text{smooth tube}}$)
PFE	energy performance factor (=$(h_D/h_p)(\Delta P_p/\Delta P_D)$)
PFS	surface performance factor (=$(h_D/h_p)(A_p/A_D)$)
Q	heat (kW)
q	heat flux (kW/m^2)
Re	Reynolds number (=$\rho Ud/\mu$)

T	temperature (K)
U	average axial flow velocity (m/s)
x	vapor quality
ΔP	pressure drop (Pa)

ABBREVIATIONS

AC	alternating current
AM	additive manufacturing
CHF	critical heat flux
CMC	critical micelle concentration
EHD	electrohydrodynamic
EHT	enhanced heat transfer
EV	electric vehicle
FMCG	fast-moving consumer goods
HTC	heat transfer coefficient ($W/(m^2 \cdot K)$)
HVAC	heating, ventilation, and air conditioning
ID	inner diameter (m)
ONB	onset of nucleate boiling
POE	polyol-ester
PVC	polyvinyl chloride
SLS	selective laser sintering

GREEK SYMBOLS

$\propto$	void fraction
β	helical angle (°)
Γ	perimeter (m)
δ	liquid film thickness (m)
ε	void fraction of vapor
θ	apex angle (°)
μ	dynamic viscosity (Pa·s)
ν	kinematic viscosity (m^2/s)
ρ	fluid density (kg/m^3)

SUBSCRIPTS

A	augmented tube
D	dimpled tube
d	inner diameter as length scale
dh	hydraulic diameter
f	liquid
g	gas
i	inner diameter
in	tube inlet
L	length as length scale
lf	liquid film
ni	plain tube
o	outer diameter

ol	outer liquid
out	tube outlet
p	plain tube
pe	pre-evaporator
r	root diameter
ref	refrigerant
sat	saturation
t	tip diameter
ts	test section
x	certain distance from inlet of tube

1.0 Introduction:

With the continuous rise and rapid growth of global industrial output, concerns related to sustainability and energy efficiency have gained significant attention in recent years. For most of these industries, the continued growth in output and productivity is directly or indirectly limited by the effectiveness of the thermal management approach. In industry, one of the most adopted techniques over which large quantities of heat are absorbed, utilizes two-phase transition from liquid to vapor and back. While there are several thermal management approaches that make use of two-phase transitions such as evaporation [1], boiling and condensation are more widely adopted due to the high levels of superheat available in industrial operations. As such, heat exchangers are used instead, and serve to facilitate heat transfer between fluid streams at different temperatures. This exchange of thermal energy is ubiquitous in many industries such as automotive, aerospace, pharmaceutical, petrochemical, and food processing [2].

By improving the efficiency of heat exchangers through heat transfer enhancement techniques, systems that are characterized by a higher gravimetric and volumetric power density can be attained. Additionally, by increasing efficiency, it is possible to produce more compact heat exchangers that are cheaper and require less raw material. This is especially vital today as overall material consumption has reached 92.1 billion tons [3]. Corollary, the carbon emissions due to transportation and production of raw material can also be reduced. This is important since the averaged mole fractions of CO_2 peaked at 405.5 parts per million in 2017 which is 147% higher than pre-industrial levels. Coupled with the decrease in material consumption, is also a decrease in waste production. This is intuitive as needing less material during production would reduce the waste produced at the end of the device lifecycle. Waste, in particular, was highlighted as a major issue in 2016, where it was reported that waste production peaked at a value of 2 billion tons [3]. Since heat exchangers are used heavily in many industries in their day-to-day operations, improving these devices would have a large-scale impact on sustainability.

Other applications for heat exchangers include air conditioning [4], where the evaporators and condensers that makeup air conditioners and HVAC&R systems are functionally similar to that of heat exchangers. Thermal management of buildings alone consumes 50% of the electrical energy production of developed nations (Fig. 1). Moreover, HVAC systems in buildings (commercial, residential, and industrial) in the United States consume around 75% of the electric power generated [5]. Furthermore, it is important to consider that even though more than one billion air conditioning units have been installed globally, the most efficient are operating at 14% of maximum theoretical efficiency. Since an additional 3.3 billion air conditioners are expected to be installed by 2050, it becomes imperative that increasing the operating efficiency is necessary. This can be achieved partly by improving heat exchanger efficiencies.

Aside from thermal management in buildings, heat exchangers also find their use in data centers where the heat generated by the electronics is absorbed by the coolant flowing in the heat exchanger tubes. Thermal management using heat exchangers, is a critical bottleneck to increasing the computational performance of modern data centers in terms of density (Gflops/m^3) and efficiency (Gflops/W)[6]. On average, about 20-30% of the energy used in modern data centers is dedicated to thermal management. In addition, server packaging density is limited by the spatial requirements of air or single-phase liquid cooling architectures [7]. By facilitating both faster clock speeds and efficient component packing than can be achieved with alternate single-phase cooling schemes, two-phase cooling approaches can improve computational density. As a result, two-phase cooling approaches have the potential to facilitate the deployment of data centers with next-generation graphical processing units for machine learning and big data analytics. This is especially important due to the persistence of COVID-19 across the globe. Many nations are requiring employees to work from home causing an increase in online information transfer and storage. The increased need for video conferencing has spurred the development and construction of multi-MW data centers which now consume up to 5% of the electrical energy generated in developed nations. This electrical energy consumption also translates into an annual increase of 6% in carbon dioxide emissions [8]. Therefore, the enhancement in thermal management would translate to less energy consumption and carbon dioxide emissions.

In addition to building energy, data center thermal management, and air conditioning, a major application requiring the use of heat exchangers is mobile systems, where radiators are the primary source for cooling. Figure 1, illustrates the breakdown of the energy consumption by the transportation sector, showing a 32% global energy consumption since 2016 [9]. Since transportation greatly contributes to carbon emissions [10], the shift towards electrified transportation is highly sought due to the significant economic and environmental benefits. However, electric vehicles (EVs) are limited by energy consumption due to cabin comfort

(HVAC) and battery thermal management[11]. Mobile HVAC systems play a very important role and can, depending on the ambient temperatures, consume up to 65% of the stored electrical energy of the vehicle's battery [12,13]. By increasing the efficiency of the heat exchangers, this energy consumption and associated carbon emissions can be reduced greatly. Consequently, key technologies are needed to design and build EVs that utilize advanced heat exchange, heat pumping, and thermal energy storage[14–16]. In addition to EV HVAC and battery thermal management [17,18], heat exchangers play an important role in large-scale water treatment applications. With 785 million people around the world lacking drinking water [3], it is imperative to develop simple water treatment methods cost-effectively. This can be achieved by highly efficient heat exchanger technology.

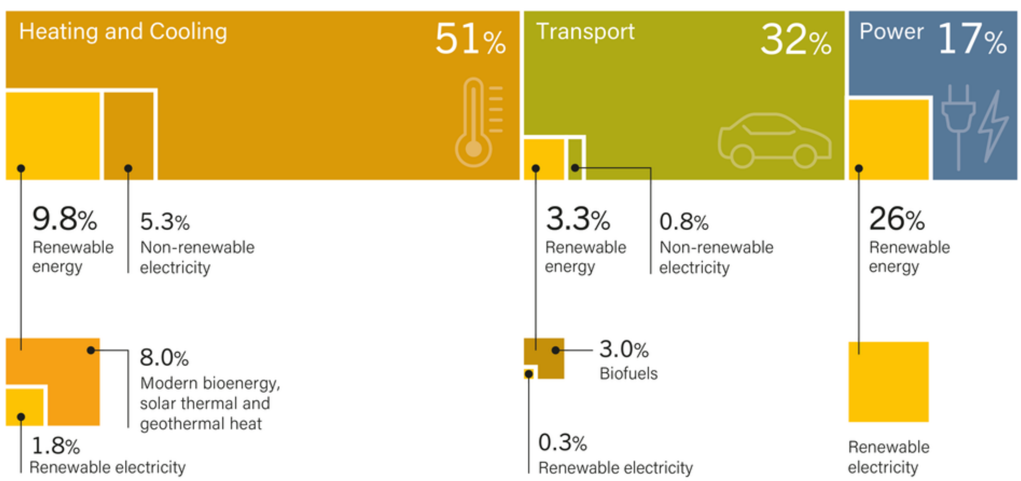

Figure 1. Total global energy consumption breakdown by sector as of 2016 [9]. Reprinted with permission from the Renewables 2019 Global Status Report, REN21, 2019, (Paris: REN21 Secretariat), ISBN 978-3-9818911-7-1. Retrieved from: 'https://ren21.net/gsr-2019'

The recent focus on renewable and sustainable energy applications such as solar-thermal power generation [19], energy storage [20], transportation electrification [21], and low GWP HVAC systems has placed a renewed interest in two-phase heat exchanger development and design [22]. From an ideal thermodynamic performance perspective, the efficiency of a heat engine increases with increasing the hot-side cycle temperature. The effort to achieve higher efficiency requires higher hot-side temperatures. In the case of sustainable closed cycle power generation systems, recent interest in the use of supercritical carbon dioxide (sCO_2) has placed added focus on heat exchanger efficiency upstream and downstream of the turbine given the harsh environments (high temperature and pressure). Hence, the development of robust and cost-effective heat exchangers could lead to substantially higher power conversion efficiencies that yield reduced fuel consumption, footprint (lower capital and operation costs), and CO_2 and NO_X emissions.

Regardless of the application, the flow in an unmixed heat exchanger can be characterized as single-phase or two-phase. While heat transfer in single-phase flow is important and has been the classical subject of interest [2], two-phase flow is complex due to the transition from liquid to vapor or vice versa. This paper focuses on two-phase flows specifically, condensation, and evaporation/boiling. While there are applications in which transition to and from the solid phase is important (e.g., reacting flows in internal combustion engines), the current review does not cover transitions to the solid phase to keep the discussion in the context of liquid and vapor phases. Furthermore, this review does not cover micro and nanoscale surface structuring[23], nor coating techniques[24] which maintain limitations owing to the lack of quantified robustness when used in realistic settings[25,26]. Table 1 presents a summary of the major applications and associated components where two-phase flow predominantly contributes to the performance of the overall system.

Table 1. Applications and components that utilize two-phase flows.

Use Category	Processes	Components	Significance of enhanced two-phase flow	Implications for energy efficiency and sustainability
HVAC&R	Air cooling	Condenser, Evaporator	Reduction in equipment size and refrigerants charge	1) Reduced cost 2) Enhanced process control 3) Improved coefficient of performance (COP) 4) Reduced environmental impact
	Air heating (heat pump)	Condenser, Evaporator		
	Refrigeration	Condenser/gas cooler, Low and medium temperature evaporator		
	Dehumidification	Evaporator		
Power Generation	Solar power generation	Energy storage system, condenser, boiler, recuperator, gas cooler	Compact system, reduction in working fluid	1) Enabling widespread implementation of modular systems 2) Reduced cost 3) Reduced environmental impact 4) Improved process control
	Fossil Fuel Based Power Generation	Condenser, boiler, recuperators, economizers		
	Nuclear power generation	Boiler, recuperators, intermediate heat exchangers for cascade cycles		
Electronics Cooling	Small scale electronics	Heat sinks, heat pipe, vapor chambers	Compact system	1) Improved performance 2) Reduced cost
	Data centers	Distributed two-phase heat exchanger, immersion cooling		
	Power electronics	Embedded heat sinks, heat exchangers		
	Electric storage, charging management	Heat sinks, heat spreaders		
Thermal Energy Storage	Thermo-chemical	Reactor for charging/discharging	Compact energy storage	1) Grid interactive systems enabled 2) Reduced cost
	Phase change materials	Embedded heat exchangers		
Miscellaneous	Waste heat recovery	Two-phase heat exchanger, heat exchangers with heat pipes	Reduced equipment size	1) Improved efficiency 2) Improved process control 3) Reduced environmental impact 4) Reduced cost 5) Enhanced fuel cell vehicle range
	Fuel cells	Integrated heat exchangers, gas reformers, vehicle radiators		
	Desalination	Evaporators/boilers, condensers		
	Renewables (wind, tidal, etc.)	Reactors (hydrogen production)		

Much of the research conducted in the past century focused on optimizing two-phase flow heat transfer in heat exchangers. This is achieved by improving the thermal performance of its heat transfer surfaces (e.g., tubes and channels). Generally, the main efforts focused on disturbing fluid flow to induce turbulence [27], enhance mixing [28], and/or maximizing the contact area between the fluid and tube walls [29]. These effects can be achieved by either geometrical modifications to the walls and/or the use of electric or magnetic fields to induce flows in certain directions [30,31].

Heat transfer enhancement techniques are classified into active and passive [31]. Passive techniques usually rely on geometrical modifications or inserts in an existing tube or channel to provide flow disturbance. Active techniques, however, rely on mechanical or electrical power input to generate oscillations or disturbances. Since passive techniques are easier and more cost-effective to implement, they are more common in the industry. However, active techniques have the advantage of providing more significant increases in heat transfer compared to passive methods. Furthermore, since the enhancement is proportional to the power input, the amount of heat transfer enhancement is controllable for active techniques.

Whether active or passive, it is important to consider the increase in pressure drop associated with the heat transfer enhancement. All techniques covered in this paper rely on disturbing the fluid flow which causes additional pressure drop along the tube. The larger pressure drop makes it necessary to use a bigger and more costly pump to compensate for the losses. If the heat transfer enhancement obtained by implementing a solution causes an excessive pressure drop, the cost penalty of using a bigger pump may overshadow the savings obtained by a more power-dense heat exchanger.

To enable a critical comparison and provide design guidelines, several enhancement factors have been developed and are summarized in this paper. However, enhancement factors should be used with caution as some may not consider the pressure drop change. This review not only presents a comprehensive summary of past enhancement techniques for two-phase flows, but it also develops design guidelines for the development of advanced heat exchangers motivated by the recent push for renewable and sustainable energy system implementation. The critical review and summary of design guidelines presented here is an important contribution given the recent advancement in topology optimization [32], machine learning algorithms[33,34], and additive manufacturing techniques being pursued for two-phase flow enhancement in internal flows [35].

2.0 Data Reduction

To identify whether a particular enhancement technique is worth pursuing, the heat transfer coefficient and the pressure drop need to be quantified. Past work can be summarized by two main experimental approaches. In this section, these two approaches are summarized.

2.1 Constant Heat Flux:

The first and the most widely adopted approach in literature refers to subjecting the test section and pre-evaporator with a known and constant heat flux. In this approach, the first step is to calculate the outlet quality of the pre-evaporator by [36]:

$$Q_{\mathrm{pe}} = C_{\mathrm{p,ref}} \dot{m}_{\mathrm{ref}} \left(T_{\mathrm{sat|pe}} - T_{\mathrm{ref,in|pe}}\right) + \dot{m}_{\mathrm{ref}} h_{\mathrm{fg|pe}}\, x_{\mathrm{out|pe}}\,, \tag{1}$$

where Q_{pe} is the heat provided to the pre-evaporator, C_{p} is the specific heat capacity of the working fluid, $\dot{m}_{\mathrm{ref}}$ is the mass flux of the working fluid, $T_{\mathrm{sat|pe}}$ is the saturation temperature at the pre-evaporator, $T_{\mathrm{ref,in|pe}}$, is the inlet temperature into the pre-evaporator, $h_{\mathrm{fg|pe}}$ is the latent heat of vaporization of the working fluid in the pre evaporator, and $x_{\mathrm{out|pe}}$ is the outlet vapor quality of the pre-evaporator. The inlet vapor quality of the test section, $x_{\mathrm{in|ts}}$, is calculated assuming:

$$x_{\mathrm{in|ts}} = x_{\mathrm{out|pe}}\,. \tag{2}$$

The test section outlet vapor quality can then be computed using [36]:

$$Q_{\mathrm{ts}} = \dot{m}_{\mathrm{ref}}\, h_{\mathrm{fg|ts}} \left(x_{\mathrm{out|ts}} - x_{\mathrm{in|ts}}\right), \tag{3}$$

where Q_{ts} is the heat provided to the test section, $h_{\mathrm{fg|ts}}$ is the latent heat of vaporization of the working fluid in the test section, and $x_{\mathrm{out|ts}}$ is the outlet vapor quality in the test section. The heat transfer coefficient can then be calculated locally at a distance, *x*, from the inlet of the test section using [37]:

$$\frac{1}{h_{\mathrm{x}}} = \frac{T_{\mathrm{wall}} - T_{\mathrm{sat}}}{q_{\mathrm{x}}} - \frac{\ln\left(\frac{d_{\mathrm{o}}}{d_{\mathrm{i}}}\right) d_{\mathrm{i}}}{2k}\,, \tag{4}$$

where h_{x}, q_{x}, T_{wall} and T_{sat} are the heat transfer coefficient, heat flux, wall temperature, and saturation temperature at a distance *x* from the test section tube inlet, respectively. k is the metal thermal conductivity of the tube, d_{in} is the inner tube diameter, d_{out} is the outer tube diameter are.

To calculate the frictional pressure drop in horizontal tubes, the following relation is used [38]:

$$\Delta P_{\mathrm{total}} = \Delta P_{\mathrm{momentum}} + \Delta P_{\mathrm{friction}} \, , \tag{5}$$

where the total pressure drop, $\Delta P_{\mathrm{total}}$, is measured experimentally, and the momentum pressure drop is calculated using the following correlation [39] :

$$\Delta P_{\mathrm{momentum}} = G_{\mathrm{ref}}^2 \left\{ \left[\frac{(1-x)^2}{\rho_{\mathrm{f}}(1-\alpha)} + \frac{x^2}{\rho_{\mathrm{g}}\alpha} \right]_{\mathrm{out,ts}} - \left[\frac{(1-x)^2}{\rho_{\mathrm{f}}(1-\alpha)} + \frac{x^2}{\rho_{\mathrm{g}}\alpha} \right]_{\mathrm{in,ts}} \right\}, \tag{6}$$

where ρ_{f} and ρ_{g} are the density of the liquid and vapor, respectively, G_{ref} is the refrigerant mass flux and α is the void fraction that can be calculated using the Steiner correlation [40].

2.2 Constant Temperature:

The constant temperature experimental approach depends on heating the test section with an outer jacket of liquid. Although this method is not as widely adopted, it is important to many studies. To calculate the heat transfer in the pre-evaporator, Eq. (1) is used. However, to compute the heat provided to the test section, Q_{ts}, the temperature change of the outer liquid jacket is used[36]:

$$Q_{\mathrm{ts}} = C_{\mathrm{p,ol}} \dot{m}_{\mathrm{ol|ts}} \left(T_{\mathrm{ol,out|ts}} - T_{\mathrm{ol,in|ts}} \right) , \tag{7}$$

where $C_{\mathrm{p,ol}}, \dot{m}_{\mathrm{ol|ts}}, T_{\mathrm{ol,out|ts}}, T_{\mathrm{ol,in|ts}}$ are the specific heat capacity, the mass flux at the test section, the temperature at the outlet of the test section, and the temperature inlet of the test section, respectively. In this case, the test section denotes the outer single-phase liquid flow jacket.

The outlet vapor quality is then computed using Eq. (3). To calculate the internal heat transfer coefficient, h_{i}, of the test section, the following equation is used [37]:

$$h_{\mathrm{i}} = \frac{Q_{\mathrm{ts}} h_{\mathrm{o}} \, A_{\mathrm{o}} \, 2\pi L k}{A_{\mathrm{i}} \mathrm{LMTD} \ln\left(\frac{d_{\mathrm{o}}}{d_{\mathrm{i}}}\right)} \, , \tag{8}$$

where $h_{\mathrm{o}}, A_{\mathrm{o}}$ are the heat transfer coefficient and surface area of the outer side of the tube, respectively. A_{i} is the inner surface area, and l is the length.

The log mean temperature difference ($LMTD$) is calculated using the following [37]:

$$LMTD = \frac{\left|\left(T_{\mathrm{ref,out|ts}} - T_{\mathrm{ol,in|ts}}\right) - \left(T_{\mathrm{ref,in|ts}} - T_{\mathrm{ol,out|ts}}\right)\right|}{\ln\left(\frac{T_{\mathrm{ref,out|ts}} - T_{\mathrm{ol,in|ts}}}{T_{\mathrm{ref,in|ts}} - T_{\mathrm{ol,out|ts}}}\right)}. \tag{9}$$

To calculate h_{o}, the single-phase fully-developed correlations developed by Gnielinski [41] and Petukhov [42] are used if the outer tube wall is smooth. Otherwise, if the tube is not smooth due to the presence of dimples or grooves, an approximation using the Wilson plot method [43,44] is used.

3.0 Heat Transfer Enhancement Techniques

This section of the review focuses on analyzing existing heat transfer augmentation techniques for two-phase flows. Two-phase flow occurs when the liquid inside a tube turns gaseous, or vice versa. Two-phase flow finds its use in many applications such as microchannel flow boiling [45], which is used to provide stream-wise temperature uniformity [46–48]. Most of the techniques reviewed within this section are passive, with one active technique (electrohydrodynamic, EHD) due to its ability to augment the heat transfer coefficient (HTC) significantly. Figure 2 summarizes the techniques reviewed.

In both boiling and condensation, the heat transfer coefficient can be enhanced by increasing the area over which heat transfer takes place[49]. However, in the case of flow boiling, the thermal resistance to heat transfer of vapor is much greater than that of liquid, so a larger wetted area inside the tube walls is preferred. Therefore, several techniques attempt to increase the possibility of annular flow inside the tube. Other techniques undertake a different approach and attempt to modify the surface (roughness) to enhance nucleate boiling. It is important to note here that although the last decade has seen a drastic amount of research effort placed on developing surface structuring techniques to enhance two-phase heat transfer for boiling[50,51], and condensation[52], the lack of demonstrated durability and long term operation (> 1 year) has precluded these methods from real industrial implementation, and hence these are not covered herein.

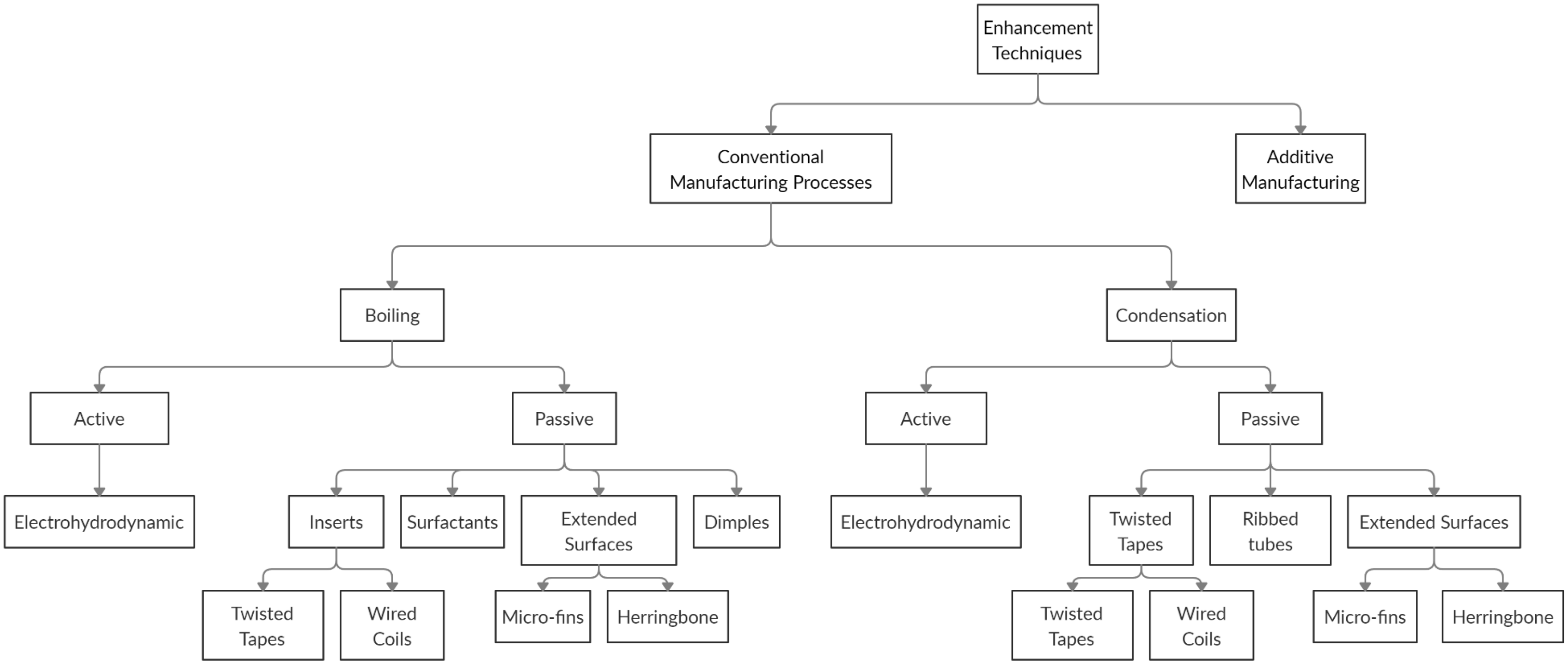

Figure 2. Summary of the enhancement techniques reviewed.

3.1 Flow Boiling:

Flow boiling is heavily used in industrial processes to absorb heat generated from operations and effectively cool down the system or the necessary working fluid. Depending on the flow rate and heat flux, the vapor quality of the fluid varies, where different qualities correspond to different flow regimes. At low vapor qualities, the bubbly flow regime is observed and nucleate flow boiling dominates. At larger qualities, the annular flow regime is observed and convective flow boiling dominates. Typically, convective flow boiling regimes are characterized by higher heat transfer coefficients and are therefore sought out. To enhance flow boiling, a common approach is to alter the surface geometry in order to create artificial nucleation sites that initiate heterogenous boiling and encourage bubble departure. This subsection investigates the effect of enhancement techniques on the in-tube flow boiling HTC.

3.1.1 Surfactants:

The first passive technique reviewed to enhance HTC in flow boiling applications is surface-active materials or surfactants. Surfactants are materials that reduce the surface tension of the liquids in which they are dissolved. Previous studies showed that small amounts of surfactant added to water can greatly enhance pool boiling [53–57]. A study carried out by Qiu *et al.* [58] investigated the effect of octadecylamine (ODA) on the flow boiling heat transfer of water in a vertical copper tube with 0.6 m length and 12 mm diameter. Using X-ray photoelectron spectroscopy, the mechanism that causes enhancement of boiling heat transfer was analyzed. When ODA is adsorbed onto the tube surface, it alters the heating of the surface which may create artificial sites for bubble initiation and growth. Furthermore, the bubble departure diameter decreases. This increases the frequency of bubble departure and in turn, enhances the heat transfer for mass fractions in the range of 1×10^{-5} to 2.5×10^{-5}. However, once the mass fraction reaches the critical micelle concentration (CMC) at 3×10^{-5} , the convective HTC decreases [58,59]. At the CMC point, the surfactants saturate the liquid-vapor interface and a new third component called micelles form in the fluid bulk. Micelles forms due to the hydrophobic attraction between the tails of the amphiphilic molecules (surfactant). When the CMC point is reached, the surface tension no longer changes and so the effect of having a higher surfactant concentration is negligible. Although HTC decreases at the CMC, there is still an enhancement when compared to flow boiling with pure water.

A study by Hetsroni *et al.* [60] investigated the heat transfer and pressure drop of water and a water-surfactant solution (*Habon G*) of 530 and 1060 ppm. The study was conducted for a fully developed laminar flow ($10 < Re_d < 450$ where $Re_d = U d_i / \nu$, where U is the average fluid speed, d is the internal tube diameter, and ν is the liquid kinematic viscosity) in a capillary tube of d_i = 1.07 mm inner diameter. It was reported that adding the surfactant would increase the pressure drop in adiabatic and diabatic flows. Furthermore, it was reported that the HTC was higher when surfactants were present.

3.1.2 Dimpled tubes:

Another passive approach taken by Shafaee *et al.* [61] highlights the heat transfer enhancement provided by dimples on a copper tube (Fig. 3). The test was carried out under specific conditions (mass flux (G) range: 155 – 470 kg/(m^2·s); vapor quality < 0.8; heat flux: 15.8 kW/m^2; saturation temperature: 56.5^{o}C, tube 9.5 mm outer diameter and 1 m length).

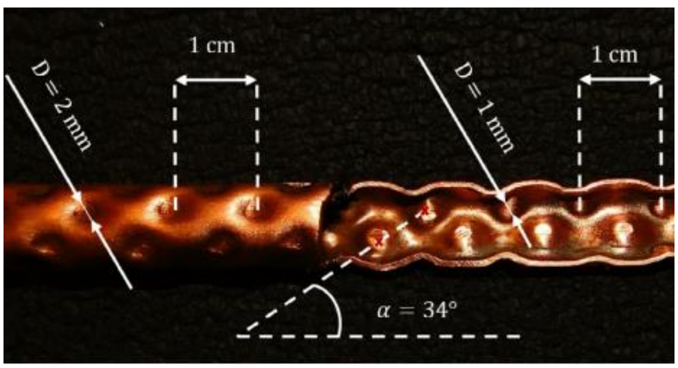

Figure 3. Image of a horizontally oriented dimpled tube [61]. Reprinted from Appl Therm Eng, 107, Shafaee et al., Evaporation heat transfer and pressure drop characteristics of R-600a in horizontal smooth and helically dimpled tubes, p. 28–36, 2016, with permission from Elsevier

The working fluid used in the investigation was R600a, as it has a lower ozone depletion potential [62,63]. The dimples in the tubes were arranged with a pitch ratio of 1.21. The dimples were of two types: shallow and deep. The diameters of the shallow and deep dimples were 1 mm and 2 mm, respectively, while the depths of the shallow and deep dimples were 0.5 mm and 1 mm, respectively.

The results for both dimple types can be categorized into two distinct regions based on the vapor quality. In the low-vapor-quality region, as the vapor quality increased, the HTC decreased, reaching a minimum between $0.15 < x < 0.45$. In the high-vapor-quality region, the HTC increased with increasing vapor quality.

Analysis of the nucleate boiling mechanism can be used to explain the behavior exhibited in the low-vapor-quality regions. For lower vapor qualities, nucleate boiling was the dominant phenomenon. However, as the quality increased and the annular flow regime initiated, the liquid in contact with the tube walls started to thin (film effect). Since the high vapor velocity carried heat away by convection, the wall superheat was reduced to a value below the minimum threshold required for bubble nucleation on the tube wall. As a result, nucleate boiling decreased, which in turn caused the HTC to decrease.

In these dimpled tubes, the range of vapor quality values over which nucleate boiling dominates was smaller than that in plain tubes. Further, the HTC increased during the low vapor quality regions. This response can be attributed to the protrusions that cause an increase in the superheated regions and thus the creation of more nucleation sites. The behavior in the high vapor quality region is due to the vaporization of the R600a refrigerant. As the refrigerant vaporized, its density decreased. The lower the refrigerant density, the higher the flow velocity, which subsequently led to liquid convection boiling dominance. Consequently, the HTC increased. For dimpled tubes, the range of high vapor quality region values over which convective boiling dominated was wider and the increase in HTC was more prominent than in plain tubes.

The experiments conducted by Shafaee *et al.* [61] showed that the HTC of dimpled tubes was 1.29–2 times greater than plain tubes. Enhanced heat transfer was observed for the dimpled tubes because they promoted swirling near the wall, which disrupted the boundary layer and increased agitation, thus promoting mixing and turbulence. Furthermore, the surface area of the tube was increased, which promoted more nucleation sites.

Mass flux also played an important role in heat transfer. When it increased, the velocity of the refrigerant increased, increasing liquid convection and the HTC. However, this influence became marginal when the vapor quality was low.

Finally, it was noted that the correlation of the HTC with Reynolds number ($\mathrm{Re_{lf}} = 4G(1-x)\delta/(1-\varepsilon)\mu_L$) was nonmonotonic. This is because, at low $\mathrm{Re_{lf}}$, smaller eddies were more prevalent. Smaller eddies had more efficient momentum transfer than larger eddies at high Re_{lf}. Therefore, the heat transfer enhancement at lower Re was smaller [64,65].

As with the other enhancement techniques, the pressure drop increased as a direct implication. Since dimples increased the frictional surface area, the frictional pressure drop in dimpled tubes was always higher than in that plain tubes, by 7–103%. This large pressure drop range can be attributed to the large vapor quality range investigated in the study. As the vapor quality of the fluid increases, the amount of vapor generated increases. Since the gaseous phase is at a higher velocity than the liquid phase due to its lower density, it imposes elevated shear stress, and hence pressure drop increases. Consequently, the pressure drop increases with vapor quality due to the velocity of the vapor growing at higher qualities. To compare the effect of dimples on the pressure drop, the pressure drop at different mass fluxes was investigated. Table 2 summarizes the findings [61].

Table 2. Pressure drop comparison between dimpled tubes and smooth tubes.

Mass flux (kg/(m^2·s))	**Pressure drop of dimpled tubes normalized by the pressure drop of smooth tubes**
420	1.1 – 1.44
305	1.07 – 1.7
205	1.27 – 1.47
155	1 – 2.03

To quantify the enhancement provided by dimpled tubes, the surface performance factor, PFS, is used [66]:

$$\mathrm{PFS} = \frac{h_\mathrm{D}}{h_\mathrm{p}}.\frac{A_\mathrm{p}}{A_\mathrm{D}}, \quad (10)$$

For all Re_{lf} values, the PFS was always greater than unity, indicating that the ratio of the convective coefficients ($h_\mathrm{D}/h_\mathrm{p}$) was larger than that of the surface area. Moreover, the convective coefficient (due to flow separation, boundary layer disruption) and the internal surface area both increased with the addition of dimples.

Although the PFS ratio does offer means of exploring the enhancement provided by dimples, it does not consider the effects of pressure drop. Another ratio, the energy performance factor, PFE [67], takes pressure drop into account. It is defined as:

$$\mathrm{PFE} = \frac{\frac{h_{\mathrm{D}}}{h_{\mathrm{p}}}}{\frac{\Delta P_{\mathrm{D}}}{\Delta P_{\mathrm{p}}}} \tag{11}$$

The PFE was calculated for different $\mathrm{Re}_{\mathrm{lf}}$ values at x = 0.173 and x = 0.45. For 60% of the PFE values, the ratio was greater than unity, indicating that the presence of dimples was favorable. The best performance, however, was at $\mathrm{Re}_{\mathrm{lf}}$ >18,000. For other $\mathrm{Re}_{\mathrm{lf}}$ values, the PFE values at x = 0.45 were greater than at x = 0.173. Consequently, annular regimes (i.e. at higher x values) are recommended.

Another commonly used correlation to quantify whether a technique is lucrative includes the thermal-hydraulic performance factor:

$$\mathrm{PEC} = \left(\frac{\mathrm{Nu}_D}{\mathrm{Nu}_0}\right)\left(\frac{f_D}{f_0}\right)^{-1/3} \tag{12}$$

Similar to PFE, PEC provides means of comparison between heat transfer enhancement and frictional pressure drop. Even though not used by Shafee *et al.* [61], PEC is one of the more popular performance correlations adopted in the field.

The arrangement of the dimple pattern influences the thermal performance. Two common designs exist in open literature: staggered and inline. Numerical simulations conducted by Li *et al.* [68] show that inline patterned dimples provide better heat transfer performance than staggered ones. The simulations also showed that the dimple shape, depth, and pitch had prominent effects on the heat transfer performance unlike other parameters such as dimple diameter. At 2300<Re<3100, it was noted that spherical dimples had the highest PEC, whereas ellipsoidal-shaped dimples had the highest PEC for Re>4000. It can be then noted that for lower Re ranges, turbulence induced heat transfer augmentation overshadows the increase in pressure drop. However, this gap is narrowed at greater fluid velocities. In all cases, it was noted that all dimple shapes have PEC>1, showing that dimples provide an enhancement of heat transfer greater that overshadows the pressure drop increase.

A study by Zahid *et al.* [69] explored the effect of dimples on a 304 stainless steel tube with 19.05 mm outer diameter, 2 m length, and a 12.75 mm diameter PVC rod insert (Fig. 4). The PVC rod was fastened with screws to ensure that it was centered. The investigation was carried over specific flow conditions (inlet saturation temperature: 5°C; heat flux: 2.5 – 15 kW/m^2; mass flux = 80 – 200 kg/(m^2·s); inlet vapor quality: 0.12–0.72). The investigation used R134a as the working fluid.

Figure 4. Photograph of a dimpled tube with PVC rod insert [69]. Reprinted from Int J Refrig, 75, Ayub et al., Two-phase pressure drop and flow boiling heat transfer in an enhanced dimpled tube with a solid round rod insert, p. 1-13, 2017, with permission from Elsevier.

As with annular flow in smooth tubes, it was noted that increasing the mass flow rate and vapor quality raised the heat transfer coefficient. Furthermore, for low mass flow rates and $x < 0.5$, there was a positive correlation between the heat flux and the HTC. However, this correlation diminished as mass velocities exceeded 80 kg/(m^2·s), at which point nucleate boiling was suppressed. The lower mass velocity behavior agreed with the observations of Tibiriçá and Ribatski [70].

Comparing the HTC of dimpled tubes containing inserts to smooth tubes with no inserts, it was noted that the HTC increased by up to threefold. Further, the pressure drop was significantly larger in tubes with inserts than that of a similar annulus region with a smooth tube. In addition, the heat transfer augmentation diminished as a mass velocity of 200 kg/(m^2·s) was approached. Consequently, as the mass velocity decreased, the HTC increased and the pressure drop decreased making the system ideal for low mass velocities. Although the insert was able to increase the HTC by up to threefold, this method had some restrictions that might render it inappropriate. The PVC insert limits the method to annular flows. However, this design could be useful for some industrial applications such as for direct expansion evaporators [69] or nuclear reactors. Moreover, to achieve the maximum heat transfer enhancement, low mass velocities are required. Otherwise, the pressure drop increases substantially and the heat transfer augmentation is reduced.

Another investigation carried out by Guo *et al.* [66], studied enhanced heat transfer (EHT) tubes produced by Vipertex (Fig. 5). These 2 m long tubes had an inner diameter of 11.5 mm with dimples/protrusions and secondary petal arrays. The modified EHT tube surface increased the surface area and flow separation, which created more nucleation sites and turbulence that disrupted the boundary layer and enhanced heat transfer. It was observed that for all three refrigerants (R22, R410A, R32), the enhancement ratio of heat transfer was 1.2 – 1.4 times larger than that for smooth tubes with a mass flux ranging between 55 and 142 kg/(m^2·s). To quantify the effectiveness of the EHT tubes, the PFS was used. In all conditions, EHT tubes provided a PFS value greater than 1, except when R32 refrigerant was used at very low mass fluxes.

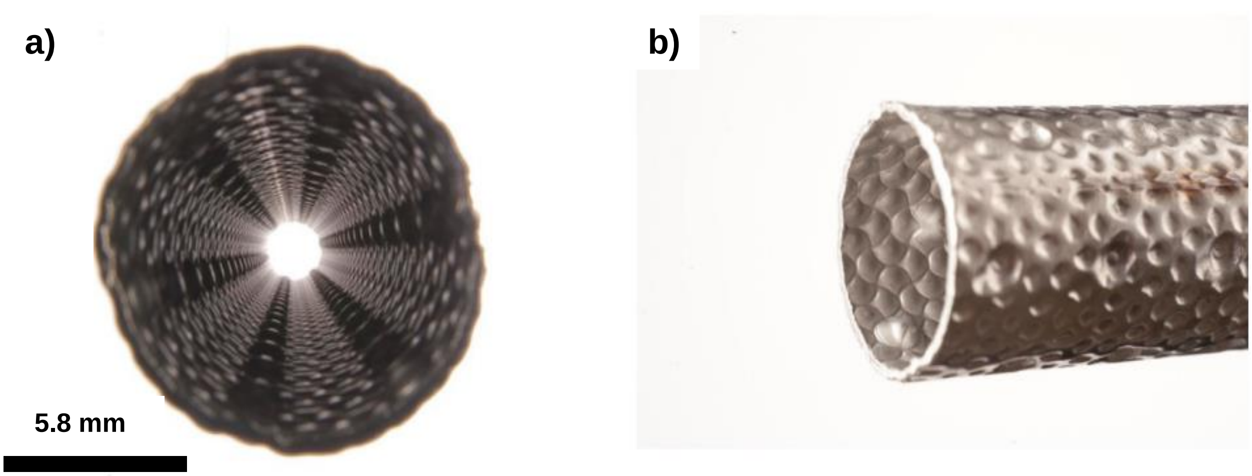

Figure 5. Photographs of EHT tubes created by Vipertex showing the (a) internal geometry, and (b) the external geometry [66]. Reprinted from Int J Heat Mass Transf, 85, Guo et al., Condensation and evaporation heat transfer characteristics in horizontal smooth, herringbone and enhanced surface EHT tubes, p. 281–91, 2015, with permission from Elsevier

Similar research by Wei *et al.* [71] examined a 2EHT tube that had both its outer and inner surfaces enhanced by longitudinal grooves with an array of dimples. Using R410A as the working fluid, the HTC of the 2EHT tubes was reported to be higher than that of smooth copper tubes by 1.11 to 1.43 times, given a mass flux range between 80 to 200 kg/($m^2 \cdot s$). Using the PFS evaluation criteria, Wei *et al.* reported that during condensation at low mass flux values, PFS was less than unity, indicating that 2EHT tubes do not provide the desired heat transfer enhancement. However, for larger flux values, it was noted that PFS is higher than 1. Contrasting these results with evaporation, it was noted that during evaporation, 2EHT tubes provided PFS greater than 1 for all mass flux values. To conclude, the 2EHT tubes provide excellent performance overall independent of which mass flux condition is used. Similar to the other studies, the dimples/embossments increased the surface area and interfacial turbulence, leading to flow separation and heat transfer enhancement between the tube wall and the working fluid.

3.1.3 Extended Surfaces:

3.1.3.1 Straight/Helical Micro-Fins:

Micro-finned tubes, first developed by Hitachi Cable [72], are commonly used in evaporator or condenser tubes due to their ability to augment in-tube heat transfer with an acceptable pressure drop penalty. Several parameters dictate the performance of micro-finned tubes including the outer diameter (d_o), root diameter (d_r), tip diameter (d_t), fin height (H), helix angle (β), and apex angle (θ). Furthermore, fins can take different shapes such as rectangular or trapezoidal. Depending on the application, the number of fins, fin height, and helix angle of the micro-fin tubes usually range between 50-70 fins, 0.075-0.4 mm, and 10°-35°, respectively [73].

By increasing the heat transfer area, micro-finned tubes can increase wetting inside the tube, which increases the rate of heat transfer. Several studies have investigated the effect of different fluids inside micro-finned tubing during flow boiling. Schlager *et al.* [74], studied the effect of 12.7 mm spiraled micro-finned copper tubes on the heat transfer and pressure drop with R22 as the working fluid. The heat transfer enhancement factor (Eq. 13) for evaporation ranged between 1.6 to 2.2. Moreover, as the HTC increased, the mass flux increased, with the HTC at 300 kg/($m^2 \cdot s$) being 400% higher than that measured at 75 kg/($m^2 \cdot s$). The pressure drop factor (Eq. 14) was lower than the EF, the maximum amounting to 1.4.

$$EF = \frac{(hA)_{\text{Enhanced tube}}}{(hA)_{\text{Smooth tube}}} \tag{13}$$

$$PF = \frac{(\Delta P)_{\text{Enhanced tube}}}{(\Delta P)_{\text{Smooth tube}}} \tag{14}$$

Using R417A, Zhang *et al.* [75] conducted flow boiling experiments in internally grooved tubes. The measured EF and PF values amounted to 1.26-2.8 and 1.8-2.6, respectively. Jiang *et al.* [76], investigated the flow boiling heat transfer and pressure drop for R22, R134a, R407C, and R410A in a 9.52 mm diameter smooth and micro-fin tube (Fig. 6). The EFs for R22, R134a, R407C, and R410A were 1.86, 1.80, 1.69, and 1.78, respectively, while the PFs were 1.42, 1.30, 1.45, and 1.40, respectively.

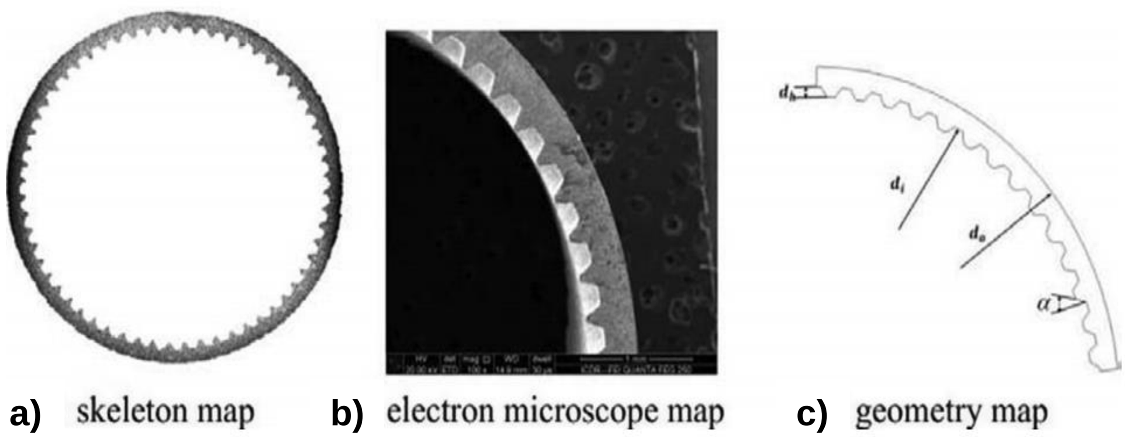

Figure 6. (a) Cross-sectional skeleton map of a micro-fin tube. (b) Scanning electron microscopy image and (c) schematic of a micro-fin tube [76]. Reprinted from Int J Heat Mass Transf, 98, Jiang et al., Experimental study of boiling heat transfer in smooth/micro-fin tubes of four refrigerants, p. 631-42, 2016, with permission from Elsevier

It is worth noting that the augmentation in heat transfer provided by the fins decreased with mass flux. This can be explained by analyzing the flow regimes inside the tube. At lower mass flux, the flow pattern in the smooth tube is stratified-wavy flow, while for the micro-fin tube, the flow regime is mainly annular. Consequently, the heat transfer in the low mass flux region is significantly enhanced. However, for higher mass flux, the annular flow pattern is present for both tubes. Therefore, the heat transfer enhancement at higher mass fluxes mainly comes from the increase in area. Several other studies were dedicated to investigating the effect of mass flux on the HTC and pressure drop. Yu *et al.* [77] studied heat transfer in a tube with helical fins having β = 18°. Using R134a, the investigation was conducted over mass fluxes between 163 and 408 kg/(m^2·s) and heat fluxes between 2,200 and 56,000 kW/m^2. The authors reported up to 200% increase in heat transfer at low mass fluxes and higher vapor qualities. Diani *et al.* [78] studied flow boiling inside micro-fin tubes with a fin height of H = 0.12 mm. Using R1234ze(E), a range of mass and heat fluxes between 375 and 940 kg/(m^2·s) and 10 and 50 kW/m^2, respectively were studied. Compared to plain tubes, finned tubes showed an average EF of 2.4 with the minimal being 1.87. The enhancement decreased with increasing mass velocity and heat flux. However, the pressure drop increased as the vapor quality increased. Using the PF evaluation criteria, it was noted that the mean value of PF is 1.4. Filho and Barbieri [79], examined the heat transfer and pressure drop of two micro-fin tubes from two different manufacturers. The fins of the two tubes had essentially the same fin geometry. Both of these tubes were compared with an equivalent smooth tube. It was noted that both finned tubes obtained the same results and both provided a significant improvement in HTC compared to a plain tube. This improvement lasted through higher mass fluxes (500 kg/(m^2·s)) and vapor qualities (x = 0.65). Since fins added flow resistance, the pressure drop in the micro-fin tubes was higher than in plain tubes. As a result, the enhancement factor for fluxes beyond 500 kg/(m^2·s) did not justify adding fins. These conclusions were drawn using PFE as the evaluation criterion. For all mass flux values below 500 kg/(m^2·s), PFE was always greater than unity (reaching a maximum of ~3 at 100 kg/(m^2·s)) for all vapor qualities. However, flux values equal to or above 500 kg/(m^2·s) started exhibiting PFE values less than unity. Kim and Shin [80] investigated seven micro-fin tubes to compare them with a smooth tube of similar geometry. For R22 and R410a working fluids, the authors calculated the PFE to be 1.86–3.27 times and 1.64-2.99, respectively, indicating that micro-fins are desirable. Dang *et al.* [81] carried out a similar investigation using carbon dioxide as the working fluid. Using a tube with fins having a helix angle of β = 6.3°, the experiment was conducted over a range of heat and mass fluxes. Similar to the results of the preceding research, it was reported that using a finned tube increased both the HTC and the pressure drop compared to a smooth tube. The HTC and pressure drop increased by 1.9–2.3 times and 1.5–2.1 times, respectively. It was noted that increasing the heat flux increases the heat transfer augmentation while increasing the mass flux decreases the augmentation.

As stated previously, the helix angle (β) is critical in micro-fin tube performance. Numerous studies have demonstrated how it affects the HTC and pressure drop in two-phase flow. Schlager *et al.* [82], examined the heat transfer and pressure drop for R22 in horizontal micro-fin tubes (9.5 mm OD) with β ranging between 15° to 25° during evaporation and condensation. The optimal angle for peak performance was shown to be at β = 25°. Oh and Bergles [83] examined the evaporative heat transfer in a 9.52 mm OD micro-finned tube with different helix angles (β = 6°, 12°, 18°, 25°, and 44°). Using R134a, it was reported that the optimal angle depended on the mass flux. The optimal helical angle for a flux of 50 kg/(m^2·s) was β = 18°, while for a flux of 100 kg/(m^2·s) it was β = 6°. Using R12, Kimura and Ito [84] studied the evaporative heat transfer in a 4.75 mm ID micro-finned tubes with β = 4°, 7°, 15°, and 30°. Similar to other investigations, it was reported that the mass flux influenced the optimal β over which heat transfer is maximized. In the stratified flow regime, the heat transfer coefficient increased with β. In the annular flow regime, the change in the HTC for β between 4° and 30° was not significant. However, within this range, the highest HTC was reported at β = 15°. Yang and Hrnjak [85] further visualized the flow patterns, over different β, in a 3D printed transparent micro-finned tube. The authors found that β affected the transition from stratified flow to annular flow where annular flow regimes occurred at lower mass fluxes and lower vapor qualities as β increased.

Most of the previous discussion was mainly focused on helical micro-fin tubes. However, axial or straight micro-fin tubes (β = 0°) are another economic option for heat transfer enhancement. Axial micro-fins are especially prevalent in aluminum tubes as they are made by extrusion. As a result, the aluminum axial micro-fin tube is considered as an alternative to copper helical micro-fin tubes in the HVAC industry. Although the heat transfer performance enhancement for axial micro-fin tubes is lower compared to helical designs, some results have shown very effective heat transfer performance in certain conditions. Chiang [86] experimentally investigated smooth, axial micro-fin, and helical micro-fin tubes having diameters of 7.5 mm and 10 mm. It was reported that the mass flux influenced the heat transfer performance in axial micro-fin tubes. When the flux exceeded 175 kg/(m^2·s), the heat transfer in the axial micro-finned tube outperformed the helical micro-fin tube. However, as the mass flux decreased to below 175 kg/(m^2·s), the helical micro-fin tube provided better heat transfer performance. Moreover, Wu *et al.* [87] concluded that the drag produced by helical angle fins had a significant effect on heat transfer at small tube diameters. Therefore, axial micro-fins had the potential for enhancing heat transfer in evaporation. Further, it was shown that, for R32, the axial micro-fin tubes increase heat transfer by 60% compared to smooth tubes.

Yang and Hrnjak [88] investigated the heat transfer and pressure drop for flow boiling in axial micro-fin tubes having a 6.3 mm ID. The tested tubes were different from previous literature (Fig. 7). In the manufacturing process, tube expansion is used to maximize the contact between the outside surface of the micro-finned tubes and the external air-side fins. This expansion process, however, changes the fin geometry and degrades the heat transfer performance. In their work, the average enhancement (EF) and pressure drop factors (PF) were 1.34 and 1.23, respectively. Yang and Hrnjak [89] further showed that the liquid refrigerant during stratified flow (especially at low vapor quality and mass flux) was easily trapped in the grooves. Moreover, since the thermal resistance of the liquid is lower than that of vapor, the heat transfer inside the tube is increased.

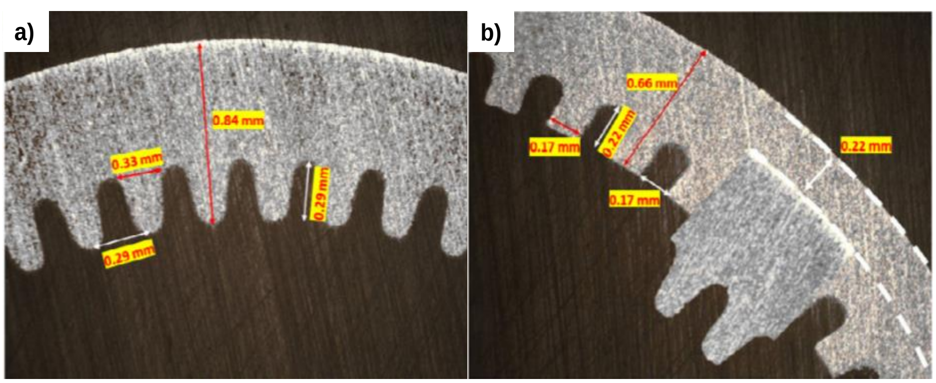

Figure 7. Cross-sectional views of: (a) unexpanded and (b) expanded axial micro-fin tubes [88] . Reprinted from Int J Heat Mass Transf, 117, Yang et al., Effect of straight micro fins on heat transfer and pressure drop of R410A during evaporation in round tubes, p. 924-939, 2018, with permission from Elsevier

3.1.3.2 Herringbone:

Another way that extended surfaces can be arranged is the herringbone pattern. The pattern mainly constitutes two sets of extended surfaces forming a V-shape. Guo *et al.* [66] investigated the effect of a 2 m long herringbone tube having an 11.43 mm fin root diameter on the HTC. The tube had a V-groove shaped pattern (Fig. 8) that carried the fluid in two different flow directions, which caused the film layer around the circumference to be nonuniform. Previous studies have proved that the structural orientation of the pattern affects the distribution of liquid around the walls and thus the HTC [90]. The study was carried out under low mass flux conditions using R22, R410A, and R32 as the working fluids.

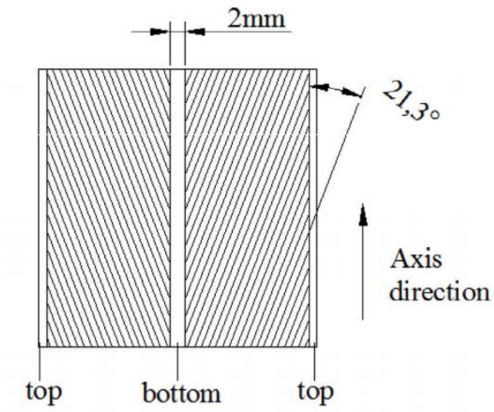

Figure 8. Schematic of a V-shaped herringbone [66]. Reprinted from Int J Heat Mass Transf, 85, Guo et al., Condensation and evaporation heat transfer characteristics in horizontal smooth, herringbone and enhanced surface EHT tubes, p. 281–291, 2015, with permission from Elsevier

The results showed negligible heat transfer enhancement in the herringbone tube. It was noted that the EF ratio (Table 5) was far less than the surface area ratio, indicating that not all inner wall areas were participating in the heat transfer enhancement. This is because sections of the tube were exposed to the vapor and so were ineffective in heat transfer. Furthermore, since the saturation temperature was lower than the condensation temperature, liquid dry-out occurred which lowered the heat transfer enhancement. This finding was highlighted using Eq. (10), which determined that the performance factor (PFS) of the herringbone tube was lower than unity during evaporation.

Similar research conducted by Olivier *et al.* [91] investigated a micro-fin copper tube (β = 18°) and compared it with a herringbone tube and a plain copper tube. The experiments were conducted over a mass flux range between 400 and 800 kg/(m^2·s) using R22, R407C, and R134a as the working fluids. It was reported that the pressure drop in herringbone tubes were 80% higher than plain copper tubes and 27% higher than micro-fin tubes. The higher pressure drop could be attributed to the fact that the surfaces extending from the tube walls prolonged the annular flow regime, which increased the vapor velocity and friction. However, unlike Guo *et al.* [66], the herringbone tube provided an enhancement in heat transfer. The average enhancement factor (PFS) was 70% higher than plain tubes and 40% higher than micro-fin tubes. Longo *et al.* [92] studied the effect of cross-grooved surfaces (Fig. 9) with a herringbone corrugation. The test was carried out with R22 as the working fluid and the results were compared to a plain tube. Repeating the experiment for a range of heat fluxes and Re_{dh} values demonstrated that the HTC increased by 1.3–1.4 times compared to a smooth surface.

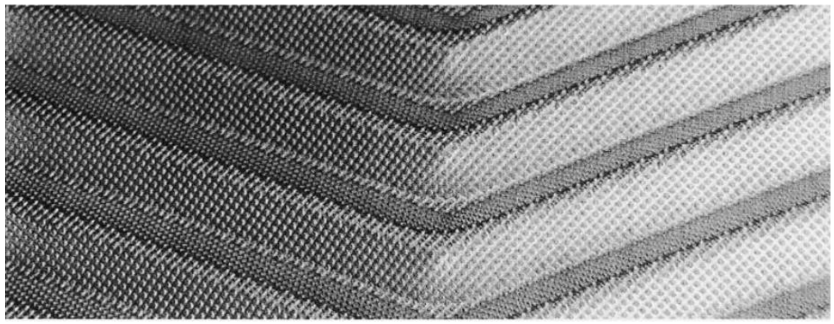

Figure 9. Image of a cross-grooved plate [92]. Reprinted from Int J Heat Mass Transf, 47, Longo et al., Experimental heat transfer coefficients during refrigerant vaporisation and condensation inside herringbone-type plate heat exchangers with enhanced surfaces, p. 4125–4136, 2004, with permission from Elsevier.

Filho and Jabardo [93] carried out experiments using R134a in herringbone and micro-fin copper tubes (Fig. 10). The experiment was conducted with a fixed heat flux of 5 kW/m^2 over a range of vapor qualities and mass flux values. It was reported that, over a wide range of mass fluxes, the herringbone tubes had superior thermal performance (PFE) compared to micro-fin tubes. However, at low mass fluxes (G = 100 kg/(m^2·s)), PFE was the lowest. Furthermore, it was noted that the pressure drop of a herringbone tube was always higher than a micro-fin tube for all mass fluxes and vapor qualities investigated. The PFE for both micro-fin and herringbone tubes was greater than unity for mass fluxes lower than 200 kg/(m^2·s). For higher mass fluxes, both tubes had values lower than unity because of the significant pressure drops observed.

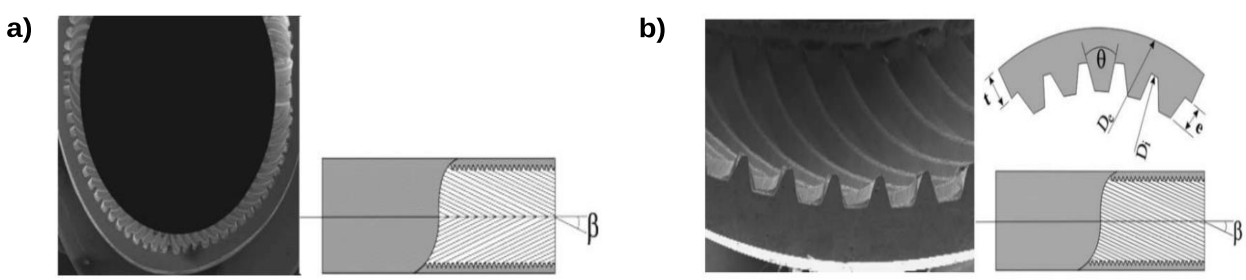

Figure 10. Scanning electron microscopy images (left) and cross-section schematics (right) of (a) herringbone and (b) micro-fin tubes [93]. Reprinted from Int J Refrig, 29, Filho and Jabardo, Convective boiling performance of refrigerant R-134a in herringbone and microfin copper tubes, p. 81-91, 2006, with permission from Elsevier

3.1.4 Inserts:

3.1.4.1 Twisted Tapes:

To increase the heat transfer coefficient in flow boiling applications, the heat transfer between the inner tube walls and the fluid must be optimized. This can be achieved by increasing the intermixing of the flowing fluid and increasing the skin contact area between the tube wall and the fluid. Twisted tapes effectively achieve both as they induce swirl flow inside the tube and act as an internal fin. To study the effect of twisted tapes on flow boiling heat transfer, Sarmadian *et al.* [94] investigated the effect of aluminum grade 6063 tapes of twist ratios 4, 10, and 15 on the heat transfer coefficient and pressure drop. Using R600a as the working fluid, the authors studied a range of vapor qualities and mass fluxes. The authors reported an increase in both pressure drop and heat transfer for tubes with inserts compared to plain tubes. Using PFE as a basis for comparison, the values ranged between 0.44-1.09. This indicated that for most of the mass flux ranges studied, the pressure drop increase far overshadowed the increase in heat transfer coefficient rendering the tape as an unviable solution. Further, it was reported that the smaller the twist ratios, the higher the HTC and pressure drop increase. A similar investigation by Kanizawa *et al.* [95] compared aluminum tapes of twist ratios 3, 4, 9, and 14 on the heat transfer performance of tubes. Using R134a, the authors repeated the experiment over a range of heat and mass fluxes. It was reported that an improvement of up to 45% in the HTC was evident in tubes with tape inserts. Accompanying this augmentation is an increase in frictional pressure drop of up to 30 times. However, the increase in the heat transfer augmentation was found to be higher than the increase in pressure drop in the majority of the operating test conditions, indicating that twisted tapes insertion is recommended. Moreover, the study indicates that the vapor quality greatly affects the performance of tubes. Vapor qualities corresponding to intermittent and annular flow witnessed an augmentation in heat transfer, while vapor qualities corresponding to even higher vapor qualities had a degradation in heat transfer. Similar patterns were observed for pressure drops where higher vapor qualities corresponded to an increase in friction. This is due to the increase in fluid velocity that occurs during liquid-vapor phase change. Shishkin *et al.* [96] also conducted a similar investigation using R134a over a range of different twist ratios, tube diameters, mass fluxes, saturation temperatures, vapor qualities, and heat fluxes. The twisted inserts used are stainless steel and are covered by a thermostable powder paint in order to electrically insulate the tape from the tube walls. It was reported that having the tape insert induced an annular flow regime at lower than usual vapor qualities. In addition, it was noted that varying the mass flux had negligible effect on the HTC for mass and heat fluxes higher than 400 kg/m^2s and 100 kW/m^2, respectively. This is due to the fact that at much higher fluxes, turbulence is already dominant and so any fluctuations in the flow velocity reap minimal changes in fluid agitation and mixing. Yan *et al.* [97] studied the effect of adding twisted tapes on the critical heat flux of highly subcooled water flowing through vertical tubes. Results show that having tapes, significantly increased the critical heat flux under high mass fluxes. Further, it was reported that the subcooled critical heat flux increased with decreasing twist ratios and vapor qualities. Additionally, it was found that increasing the mass flux increases the critical heat flux, however, this effect is dampened at regimes near the saturation point.

3.1.4.2 Wired Coils:

Similar to twisted tapes, wired coils help agitate flow to enhance fluid intermixing. However, this agitation is more focused on the boundary layer near the tube wall. To study the effect of wired coils on the heat transfer and pressure drop, Behabadi *et al.* [98] inserted coils of different diameters and pitches in a 1.2 m long copper tube with an inner diameter of 7.5 mm. Using R134a as the working fluid, it was reported that having a coil insert can cause a pressure drop increase of up to 1000% when compared with plain tubes with no insert. Further, the enhancement of heat transfer was found to depend on the vapor quality, with the maximum enhancement in HTC peaking at 98%. Moreover, it was noted that the HTC increased with decreasing coil pitch up to a minimum of 8 mm. Further reduction in pitch would cause a decrease in the HTC as the insert resists heat transfer like a solid shell [99]. Since the pressure drop caused by the inserts is much higher than the increase in HTC, it was concluded that having wired coils is not favourable. Niezgoda-Żelasko [100] investigated wired coils of different pitches and diameters at a range of mass and heat flux values in vertical tubes. Using R507, R410, and R407C as the working fluid, the HTC for azeotropic fluids increased by 1.1-1.7 times, while the HTC for zeotropic agents increased by 1.1-1.3 times. Further, the pressure drop also increased by 1.8-4.5 times when compared to plain tubes. Alimardani *et al.* [101] conducted a similar study but with R600a as the working fluid. Using horizontally oriented tubes, the authors noticed an increase in pressure drop by 90-958% when wired coils were inserted. However, this pressure drop is reduced when the wire diameter decreases, and the coil pitch increases. Additionally, the authors reported *PFE* values ranging between 0.13-1.4. Yun *et al.*[102] investigated wired coil inserts in tubes with nitrogen fluid. Using different wire pitches and diameters, the authors conducted experiments over a range of mass and heat fluxes. The wired coils augmented the HTC and pressure drop. It was noted that an increasing mass flux and decreasing heat flux caused an increase in the HTC. The pressure drop was also found to increase with decreasing mass flux. Generally, for the investigated range of mass flux values, Yun *et al.* reported PFE values greater than unity indicating that wired coils are an effective method to augment heat transfer. From the above studies, it can be concluded that due to the high pressure drop that characterize wired coil inserts, this heat transfer enhancement technique is only viable in very limited applications and test conditions.

3.1.5 Electrohydrodynamics:

The final enhancement technique to be covered in two-phase flow boiling is an active method. In this method, dielectric fluid is subjected to an electric field to induce motions in certain directions. Like dimples and extended surfaces, electrohydrodynamics (EHD) can augment heat transfer in both single-phase flow and two-phase flow boiling.

For two-phase boiling, EHD can augment heat transfer in several ways. First, it is known that for low heat flux values, heat is transferred through forced or natural convection. As the heat flux or superheat increases, the *onset of nucleate boiling* (ONB) [38] occurs and some nucleation sites are activated. Applying EHD has been shown to initiate ONB at an earlier stage (*i.e.*, at a lower wall temperature) and eliminate the hysteresis portion that occurs before ONB [103–106]. EHD also raises the critical heat flux (CHF) limit, and eliminates the heat flux drop between CHF and film boiling [103,107]. Moreover, when an electric field is applied, the surface tension of the dielectric fluid is lowered which increases its wettability on the surface [106,108] and enhances the heat transfer in a way similar to surfactants. Finally, since the frequency of bubble departure increases, the turbulence induced by the bubbles rising aid heat transfer [104,109,110]. Additionally, it is important to note that the inner walls of the tube surface have a prominent effect on heat transfer enhancement [103,111,112].

Cotton *et al.* [113] investigated the effect of EHD on the heat transfer of R134a in an annular channel under various mass fluxes and voltages. It was noted that at 24 kV and 60 Hz AC, the average HTC and pressure drop increased by 300% and 260%, respectively. This increase in heat transfer was attributed to the oscillation in flow which caused intermixing between phases and increased the interfacial area. Further, Cotton *et al.* [114] experimentally and numerically studied the impact of the electric field and the electrode position inside the tube. Using R134a as the working fluid, the experiment was carried out over a range of mass fluxes, vapor qualities, and voltages for three different electrode positions, mainly at the center and ± 2.73 mm from the centerline of the tube. It was found that heat transfer was enhanced by up to 60% compared to a tube with no electric field. Furthermore, the pressure drop increased by only 20%. There was also a positive correlation between the heat transfer augmentation and the applied voltage. However, this augmentation decreased with increasing mass flux. Using R134a, Salehi *et al.* [115] investigated EHD enhanced flow boiling inside a 1 mm round tube. The experiment was repeated twice for smooth and corrugated tubes over a range of voltages, Re_{dh} values (where $Re_{dh}=4\dot{m}/\Gamma\mu$), flow directions, and vapor qualities. It was reported that the technique was most effective at lower Re_{dh} values. For Re_{dh} = 500, the boiling HTC increased tenfold when a 3 kV potential was applied over the corrugated tube with downward flow. Liu *et al.* [116] investigated the impact of electrode polarity on EHD heat transfer augmentation in a vertical tube. Using R123 as the working fluid, the electrode, carrying high negative or positive voltages, was placed concentric to the stainless-steel tube. The results showed that positive high voltages resulted in superior heat transfer enhancement and required lower electric field strength. The maximum enhancement factor amounted to 20.1 for an electric field strength of 1333 kV/m. Applying an electric field to a vertical tube created a dielectrophoretic force that pushed on the bubbles forming against the tube wall. This caused the bubbles to deform and spread along the surface which accelerated bubble growth by increasing the area of liquid film underneath the bubbles for evaporation. Furthermore, the force that caused thinning in the liquid film, increased the proportion of the bubbles in the superheated boundary layer, and increased the surface area per unit volume of the bubbles. However, if the intensity of the field increased above a certain threshold, the force acting on the bubbles would increase to the extent that bubbles would not be able to depart from the tube walls, preventing new liquid from replacing the gas and in turn reducing the HTC. Besides, a positive charge had the effect of increasing the body force on bubbles close to the surface causing an enhancement in heat transfer, while a negative charge had the opposite effect.

Compared with the passive techniques discussed above, a clear advantage that can be noted is the ability of EHD to enhance and affect every part of the boiling curve, in contrast to passive techniques that only aim to enhance the nucleate boiling region [103]. Furthermore, it can be noted how capable EHD is in enhancing HTC. However, active methods are not used as frequently as their passive counterparts due to the complexity such methods add.

3.2 Condensation:

The main challenge in condensation heat transfer augmentation techniques is the removal of liquid condensate from the walls of the condensing surface as soon as they form [117,118]. As liquid condenses on the surface and the thickness of the liquid film increases [119], the thermal resistance to heat transfer from the vapor to the surface increases [120,121] which hinders heat transfer [122]. This subsection is dedicated to investigations that study the effect of tube enhancements on the HTC in the case of two-phase flow condensation.

3.2.1 Inserts:

3.2.1.1 Twisted Tapes:

As highlighted, a twisted tape insert can enhance heat transfer through several means. Firstly, a twisted tape restricts the fluid to flow along the twisted pathway, which increases the flow length. Furthermore, a twisted tape serves as a fin, which increases the area of contact between the tube and the flowing fluid. Moreover, having a twisted tape also induces swirl mixing, which induces turbulence and vortices [123]. The increase in the axial velocity and the creation of vortices by the tapes aid in increasing the vapor shear effect and the condensate entrainment, which leads to further enhancement in HTC [124]. However, it is noted that using twisted tape inserts to enhance heat transfer adds obstruction to the fluid flow, and thus results in a significant pressure drop. Using R134a as the working fluid, Hejazi *et. al* [125] investigated the impact of a twisted tape on the in-tube heat transfer during condensation. The results revealed that twisted tape inserts enhance the HTC but also increases the pressure drop. Under the worst test conditions, the pressure drop experienced was 2.4 times more than that in a smooth tube. However, under the best test conditions, the condensation HTC increased by up to 40%. Overall, it was proven that the additional pressure drop attributed to the twisted insert was so large that it did not justify the use its use. Akhavan-Behabadi *et al.* [126] examined the condensation heat transfer in tubes with twisted tape inserts of various twist ratios. Using R134a as the working fluid, it was reported that the HTC increased with the mass flux, while the twist ratios had a negligible effect. In addition, at low mass fluxes, the HTC was reported to increase by up to 38%. Agrawal *et al.* [127] studied the heat transfer augmentation provided by segmented and full-length twisted tape inserts. Using R22 as the working fluid, different mass fluxes were investigated. The enhancement in heat transfer during condensation was found to reach up to 25% for a full-length twisted tape insert. Although segmented twisted tapes also caused an enhancement in the HTC, it was reported to be relatively small. This enhancement improved with increasing the length of the segmented tape and was maximum for the full-length tape inserts. Furthermore, the authors reported that all the tape inserts were generally more effective at low mass fluxes. At higher mass fluxes, the axial velocity of the fluid is high and so the added enhancement provided by the tape in the flow field becomes inconsequential. In general, it is apparent that the HTC increases with the increase of segmental length and is the highest for the full-length tape inserts. However, it was reported that the full-length tape insert remained effective at the higher mass flow rates as well.

3.2.1.2 Wired Coils:

Another type of widely used inserts is wired coils. Acting as added roughness, wired coils disturb the boundary layer of the fluid near the tube walls. This causes an enhancement in heat transfer in addition to pressure loss. Agrawal *et al.* [128] investigated the effect of a coiled wire on the condensation of R22 inside a horizontal tube. The investigation spanned over a range of wire diameters and coil pitches. Results reveal that having a wired coil insert could increase the condensing HTC by as much as 100%. Further, the HTC enhancement increased with wire diameter for high vapor qualities and vice versa for low vapor qualities. At high vapor quality, the liquid film thickness on the inner walls of the tube decreased, which lowered the thermal resistance. Similar observations were exhibited for tubes with micro-fins and twisted tape inserts [129,130]. Furthermore, for a given wire diameter and low vapor quality, the heat transfer enhancement increased as the coil pitch decreased. To study the pressure drop associated with such an insert, Akhavan-Behabadi *et al.* [131] studied a double-pipe heat exchanger with R134a as the working fluid. Coils of different diameters and pitches were experimentally studied. It was reported that using a coiled wire insert increased the pressure drop by 260–1600% compared to a plain tube with no insert. Moreover, the pressure drop decreased with decreasing wire diameter and increasing wire pitch. A similar investigation of pressure drop due to coiled wires was conducted by Salimpour and Gholami [132]. Using R404A, the experiment was carried out over a range of mass fluxes and vapor qualities. A pressure drop increase of up to 1300% was observed compared to smooth tubes. This pressure drop was reported to increase with coil diameter and reduced coil pitch.

3.2.2 Ribbed tubes:

Ribbed tubes or corrugated tubes, like coiled wires, add roughness that disturbs and limit the growth of fluid boundary layers. Laohalertdecha and Wongwises [133] studied the effect of corrugation pitch (Fig. 11) on the HTC. The R134a condensation experiments were conducted with three tubes of different corrugation pitches (5.08, 6.35, and 8.46 mm) at different saturation temperatures, heat, and mass fluxes. The study found that the average HTC and pressure drop increased with mass flux and vapor quality. Furthermore, increases of up to 50% and 70% in the HTC and frictional pressure drop, respectively, were shown for corrugated tubes. Khoeini *et al.* [134] studied the effect of inclination ($-90^{\circ} \leq \propto \leq +90^{\circ}$) on the heat transfer of R134a inside a corrugated tube. The results showed that at lower velocities and vapor qualities, the highest heat transfer augmentation was achieved at an inclination of +30°. This was 1.27–1.41 times greater than the worst achieved heat transfer augmentation occurring at −90°. The latter had the lowest heat transfer performance since the interfacial shear stress and the gravity forces both acted together. As a result, the flow remained annular. The thickness of the condensed liquid on the wall increased, increasing the thermal resistance, which caused a decrease in heat transfer. Fernández-Seara and Uhía [135] studied the condensation of ammonia on spirally corrugated tubes. The setup constituted of a heat exchanger with water inside the corrugated tube and ammonia surrounding the outside of the tube. The experiment was carried out over a range of wall subcooling values, and it was reported that the overall performance for corrugated tubes was 1.27 times higher than plain tubes. However, the enhancement factor of the condensing HTC turned out to be close to unity over the range of wall subcooling temperatures tested.

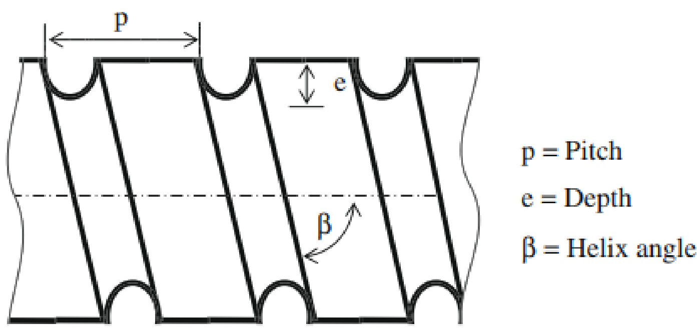

Figure 11. Side-view schematic of a corrugated tube [133]. Reprinted from Int J Heat Mass Transf, 53, Laohalertdecha and Wongwises, The effects of corrugation pitch on the condensation heat transfer coefficient and pressure drop of R-134a inside a horizontal corrugated tube, p. 2924-2931, 2010, with permission from Elsevier.

3.2.3 Extended Surfaces:

3.2.3.1 Micro-fins:

Fins enhance the condensation HTC because they increase the surface area as well as the tendency of thin-film condensate to form on their tips [31]. Jung *et al.* [136] examined the effect of micro-fin tubes on the flow condensation HTC for a range of mass and heat fluxes. Using R22, R134a, R407C, and R410A as the working fluids, it was reported that using micro-fin tubes caused a twofold to threefold rise in the HTC compared with smooth tubes. This enhancement, however, decreased with increasing mass flux. These results matched another investigation by Kwon *et al.* [137], who studied the condensation in a micro-fin tube. Using R22 and R410A, the setup consisted of a counterflow heat exchanger where the refrigerant flowed inside the finned tube and the cold water flowed outside of the tube. Carried over a range of mass fluxes, the enhancement ratio of the finned tube increased by 1.5 to 2.2 times based on the nominal heat transfer area. This enhancement was found to negatively correlate with the mass flux. Eckels and Pate [138] conducted their investigation with a tube containing 60 fins with 0.2 mm height and 17° spiral angle. Using R134a and CFC-12 as the flowing fluids, the study was conducted over a range of mass fluxes and wall temperatures. Using the fins provided a positive effect on the heat transfer for both refrigerants. For HFC-134a, it was noted that the HTC during condensation increased by 1.75–2.5 times that of smooth tubes. In the case of R12, the increase was 1.7–2.3 times. Accompanying this enhancement was also an increased pressure drop. However, it was noted that in almost all cases, the increase in HTC overshadowed the pressure drop increase. In consequence, having micro-fins proved to be an effective heat transfer enhancement technique. Similarly, Naulboonrueng *et al.* [139] carried out their investigation using R134a as the working fluid. A 2.5 m long tube containing micro-fins was subjected to temperatures between 30°C and 40°C. It was reported that the HTC during condensation was 1.1–1.85 times higher than that of smooth tubes because the micro-fins promoted mixing. This HTC enhancement increased with higher quality and mass flux. Further, Naulboonrueng and Wongwises [140] went on to investigate the pressure drop in the same micro-fin tube using the same refrigerant. It was reported that the disturbance in the fluid flow caused by the micro-fins increased the pressure drop by 10–50% compared with a smooth tube. Moreover, the pressure drop increased with vapor quality and mass flux. Finally, Graham *et al.* [141] investigated, over a range of mass fluxes, the effect of axially grooved tubes on the condensation of R134a and compared it with the performance of helically grooved tubes (β =18°). The extent of heat transfer enhancement was dependent on the mass flux and quality ranges. For mass fluxes of 150 kg/(m^2·s), axially grooved tubes provided better thermal performance than helically grooved or smooth tubes. However, the pressure drop for the axially grooved tubes was similar to that for helically grooved tubes, and the pressure drop for both was higher than that of plain tubes.

Eckels *et al.* [142] studied the use of 150 SUS pentaerythritol ester lubricants in a micro-fin tube. The tube contained 60 fins with 18° spiral angles. Using R134a, Eckels *et al.* reported that the condensation HTC and pressure drops were 50–200% and 10–50% higher, respectively than smooth tubes. The increase in heat transfer was adversely affected by higher lubricant concentration, while the pressure drop was unaffected. A similar investigation by Cho and Tae [143] used polyol-ester (POE) and mineral oils instead of the ester lubricant. R22 and R407C were used as the working fluids, and the experiment was extended to tubes with U-bend sections. The experiment was conducted over a range of oil concentrations, mass fluxes, and inlet vapor qualities. For straight sections before the bend, it was reported that the oil concentrations adversely affected the heat transfer augmentation since it increased the viscosity of the flowing fluid. In the U-bend section, the heat transfer augmentation was reported to be at maximum value. The enhancement was attributed to the fact that the U-shape bend promoted secondary flows and flow disturbances. Moreover, the straight section following the bend showed a higher average HTC than the straight section preceding the bend. This is because the secondary flow and disturbances occurring at the bend extended to the straight section after the bend. Finally, the pressure drop was also reported to increase with oil concentration.

3.2.3.2 Herringbone:

Miyara *et al.* [144] examined how herringbone patterns affected the condensation of R410A and R22 and compared it with conventional helical micro-fin tubes. The authors reported that for high fluid velocities, the performance of the herringbone pattern was superior to that of the helical micro-fin tube. However, at low velocities, the opposite was true. In general, herringbone tubes were able to collect liquid flowing at the top and bottom sections of the tubes. Consequently, the liquids left at the sides of the tubes were much thinner, enhancing heat transfer. Moreover, like conventional helical fins, herringbone tubes promote turbulence and mixing which enhances heat transfer. Finally, regardless of the velocity, the herringbone micro-fin tube always had a pressure drop larger than that of the helical fin tubes. Miyara *et al.* [145] went on to study the effect of the fin shape on the herringbone-patterned extended surface. The study was conducted using R410A. Results show that longer fins led to an increase in heat transfer. However, this enhancement had a plateau when the fins reached a length of 0.18 mm. Furthermore, it was reported that the HTC increased with higher helix angles. This was attributed to the fact that more-helical fins increased the circumferential force acting on the liquid which affects the film thicknesses. Although changing the fin shape augmented the heat transfer enhancement, the pressure drop increased with the fin height or helical angle. Goto *et al.* [146] investigated herringbone grooves and spiraled grooves (Fig. 12) and their effect on the heat transfer coefficient. Using R410A and R22, the investigation was conducted over a range of mass fluxes. It was reported that herringbone grooves provided twice the increase in HTC compared with spiraled grooves. The heat transfer enhancement was due to the enhanced mixing of the liquid film of refrigerant in addition to the increased surface area for heat transfer. Further, Goto *et al.* [147] conducted a similar experiment with R410A and R22 at a different range of mass fluxes and pressures. The results of this investigation agreed with the results of the previous Goto *et al.* study showing twice the HTC in herringbone tubes compared with helical tubes [146].

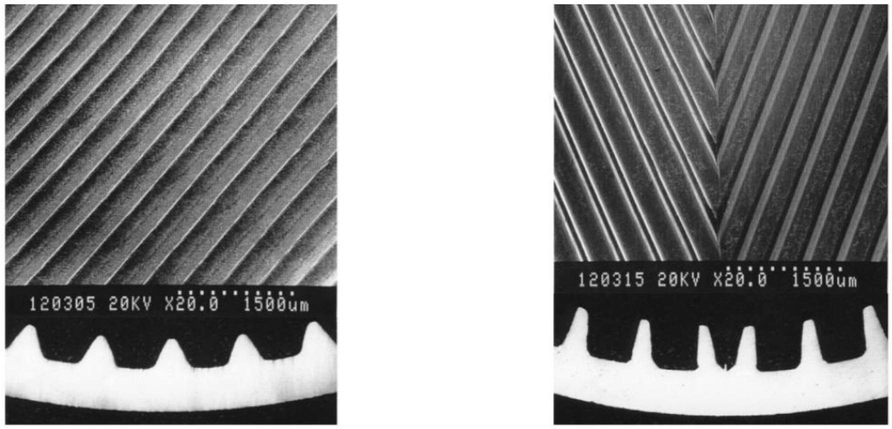

a) Spiral grooved tube (C Tube) **b)** Herring-bone grooved tube (W Tube)

Figure 12. Scanning electron microscopy images of (a) spiral grooves, and (b) herringbone grooves [146]. Reprinted from Int J Refrig, 24, Goto et al., Condensation and evaporation heat transfer of R410A inside internally grooved horizontal tubes, p. 628-638, 2001, with permission from Elsevier.

3.2.4 Electrohydrodynamics:

When condensation occurs, the least volatile substances condense first. As time passes, the concentration of volatile liquids in the vapor increases to the extent that a concentration gradient arises between the vapor near the free surface and the bulk flow. Consequently, diffusion starts to occur which obstructs the flow of any condensing vapor and so decreases the heat transfer due to the increase in interfacial resistance. EHD is used to reduce this resistance and augment the heat transfer [148]. Gidwani *et al.* [148] examined the effect of EHD using R134a, R407c, and R404a. The experiment was conducted with smooth and corrugated tubes. Using R404a, results showed that the use of an 18 kV electric field enhanced the heat transfer performance by 18.8 times for smooth tubes, and increased the pressure drop by 11.8 times. Repeating the experiment for corrugated tubes, the heat transfer enhancement reported was 5.8 times. For R134a, the maximum heat transfer augmentation inside a corrugated tube was reported to be 8.3 times higher than that in a smooth tube, and the pressure drop was 20.8 times higher. Finally, for R407c, the heat transfer increased by 3.9 times and 2.9 times for smooth and corrugated tubes, respectively. An increase in HTC was also reported by Choi [149]. Using R113 as the working fluid inside a vertical tube, a radial DC field was applied. The electric field caused increased the thinning of the liquid film, causing the condensing HTC to increase. For an applied voltage of 30 kV, an increase on the order of 100% was reported for the condensing HTC downstream of the tube. Didkovsky and Bologa [150] investigated the effects of electric fields of different strengths, frequencies, and uniformities on the condensation of stagnant water vapor inside a tube. It was reported that the HTC increased by 20 times compared with no electric fields. This was attributed to the thinning of the film layer in the recesses between transverse waves.

4.0 Advanced Manufacturing Processes for Two-Phase Flow Enhancement

In the previous subsections, techniques to enhance two-phase flow in channels were presented. However, despite extensive developments in the active and passive enhancement techniques mentioned above, there are major limitations for the maximum achievable performance due to constraints in channel design that stem from production using conventional manufacturing processes. Recent developments in additive manufacturing, however, provide unprecedented solutions in the form of extremely complex configurations for thermal management [20,151,152]. For example, the deployment of a structure with a controlled feature size has been made possible due to three-dimensional printing technology[153]. As illustrated in Fig. 13, the diameter of the copper sphere can be varied providing an effective technique for enhancing the boiling process due to continuous contact of liquid on the hot surface [154]. To date, there are several experimental studies to enhance pool boiling heat transfer coefficient by deploying porous structures and structural modifications [155,156].

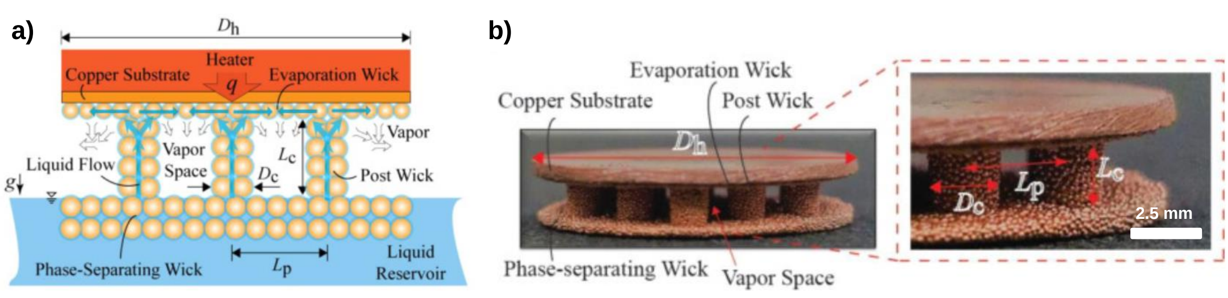

Figure 13. Wicking structure for enhanced boiling heat transfer developed by sintering of copper spheres where: (a) Schematic and (b) Fabricated sample [154]. Reprinted from Int J Heat Mass Transf, 155, Egbo et al., Phase-change heat transfer of sintered-particle wick in downward facing orientation: Particle size and wick thickness effects, 119840, 2020, with permission from Elsevier

For example, Ho *et al*. [157] conducted an experimental investigation to enhance the pool boiling heat transfer performances of surfaces with microcavities and micro-fins fabricated by the SLM (selective laser melting) technique (Fig. 14a). Using FC-72, an improvement of around 70% was reported in the average HTC as compared to a plain Al-6061 surface. In another investigation, Wong *et al*. [158] studied the effect of porous structure thickness. Approximately threefold enhancement was shown in the HTC and an improvement of a similar order for the CHF compared to a plain surface (Fig. 14b-d). It is important to note that despite being an active area of research, there are obvious discrepancies in findings. For example, Rainey and You [159] prepared samples using additively manufactured samples and demonstrated noticeable improvement in the HTC. However, in another study with similar experimental arrangements, Kim *et al*. [160] observed a relatively lower improvement in the HTC. It was further reported that under certain conditions, the samples manufactured by additive manufacturing showed reduced performance compared to the baseline case. Overall, there is a consensus that when designed appropriately and fabricated with reasonable dimensional accuracy, the sample produced by additive manufacturing can lead to a remarkable increase in thermal performance. Regardless of the extensive developments, it is important to note that most of the research and development work in the field of two-phase heat transfer using additive manufacturing has been focused on pool boiling.

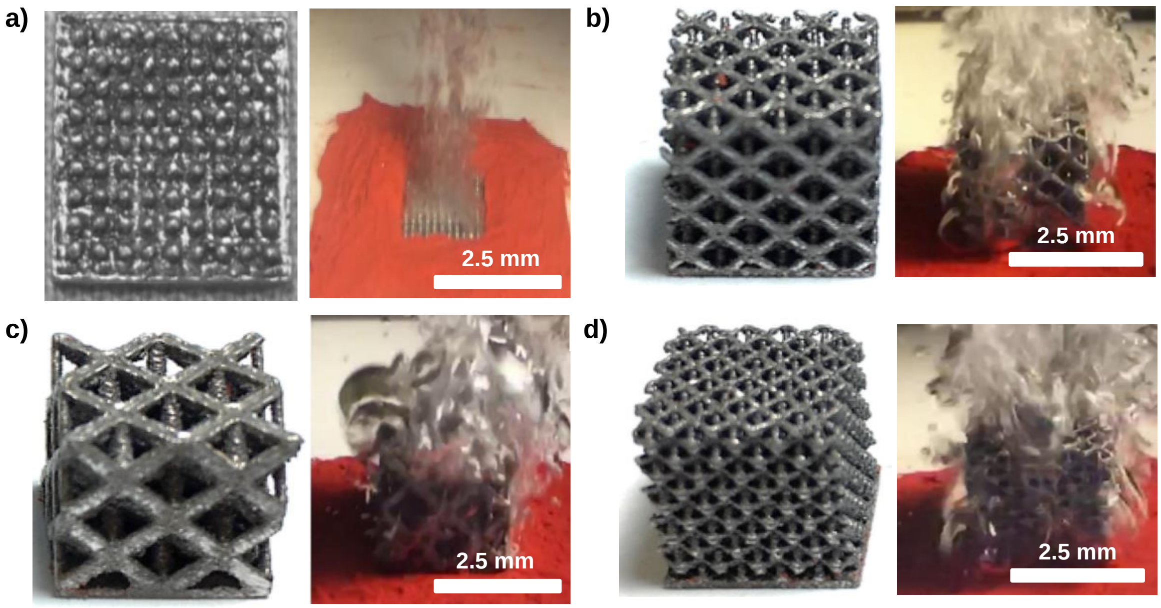

Figure 14. (a) micro-fin array of fin size of total surface area size of 1.35 cm^2 with pool boiling [157]. Adapted from Int J Heat Mass Transf, 99, Ho et al., Saturated pool boiling of FC-72 from enhanced surfaces produced by Selective Laser Melting, 107-21, 2016, with permission from Elsevier. Porous structures in pool boiling setup where: (b) Unit cell size 2.5 mm with dry-out boiling, (c) Unit cell size 5.0 mm with dry-out boiling, (d) Unit cell size 10.0 mm with water replenishment [158]. Adapted from Int J Heat Mass Transf, 121, Wong and Leong, Saturated pool boiling enhancement using porous lattice structures produced by Selective Laser Melting, p. 46-63, 2018, with permission from Elsevier

The applications where advanced manufacturing has led to extensive enhancement in thermal-hydraulic performance for two-phase flow include heat pipes, heat sinks, and heat exchangers [161]. Heat pipes have been studied extensively due to the special feature of dispersing heat over large distances. Due to the nature of the operation, two major issues with conventional heat pipe technology include the dependence of dissipation rate on the design/characteristics of the wicking structure and the limited flexibility to adopt complex geometries. Both issues have been effectively resolved by additive manufacturing since the advanced processes can produce porous wicking structures with varying levels of complexity and feature sizes [162–166]. Further, it has become possible to embed heat pipes to the applications under consideration regardless of the complexity of the shape. Some examples of the deployment of porous structures in heat pipes are presented in Figure 15.

+

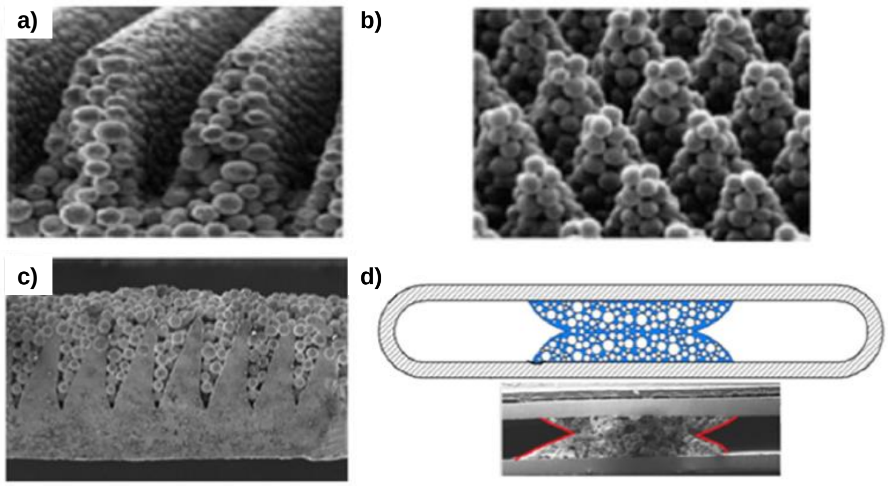

Figure 15. SEM imaging of 2-D and 3-D modulated porous coatings of height: (a) 1.7 mm and (b) 1.2 mm [162]. Reprinted from Int J Heat Mass Transf, 52, Min et al., Kaviany M. 2-D and 3-D modulated porous coatings for enhanced pool boiling, 2607-13, 2009, with permission from Elsevier. (c) SEM imaging of wick with sintered spherical powder of 75-110 μm diameter [164]. Reprinted from Int J Heat Mass Transf, 56, Deng et al., Characterization of capillary performance of composite wicks for two-phase heat transfer devices, p. 283-293, 2013, with permission from Elsevier. (d) Ultra-thin heat pipers and SEM imaging of the wick structure [166]. Adapted from Appl Therm Eng, 86, Li et al., Investigation of ultra-thin flattened heat pipes with sintered wick structure, p. 106-118, 2015, with permission from Elsevier

Ameli *et al*. [167] carried out an investigation on ammonia-based heat pipes fabricated using AM of aluminum alloy. The investigation focused on the characterization and deployment of wick structures of different porosities, thicknesses, pore sizes, and permeabilities in different regions of a heat pipe to maximize the performance (Figure 16).

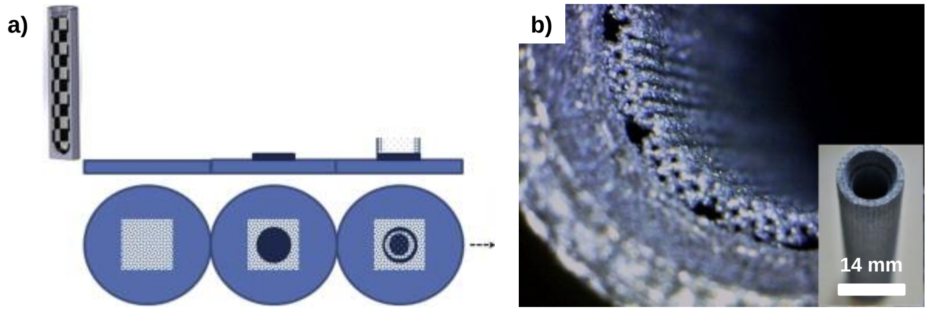

Figure 16. (a) Fabricated HP by SLM and (b) Close-up to arterial wick fabricated through SLM [167]. Adapted from Appl Therm Eng, 52, Ameli et al., A novel method for manufacturing sintered aluminum heat pipes (SAHP), p. 498-504, 2013, with permission from Elsevier

In another experimental study, Esarte *et al*. [168] designed a linear heat pipe where selective laser sintering process (SLS) was used for the fabrication of the primary wick. The heat pipe was utilized to manage the heat produced from a Light Emitting Diode lamp. The hydraulic-thermal limits for such a system were established based on design parameters such as permeability, capillary pumping, and wettability of the system. Similarly, Thompson *et al*. [169] utilized an additive manufacturing process to manufacture a compact flat-plate oscillating heat pipe. The heat pipe, made of Ti–6Al–4V, was shown to exhibit a thermal conductivity of approximately 110 W/m K at a power input of 50 W which was reported to be 400–500% higher compared to the thermal conductivity of solid Ti–6Al–4V. Follow-up work conducted by Ibrahim *et al*. [170], a multi-layered Ti-6Al-4V based oscillating heat pipe was fabricated with improved design (Fig 17). The performance of the heat pipe was assessed at different power inputs where the neutron imaging facility at Oak Ridge National Lab was used to observe the behavior of two-phase flow in channels. Additionally, different fluids including n-pentane, NovecTM 7200, acetone, and water were used in the study.

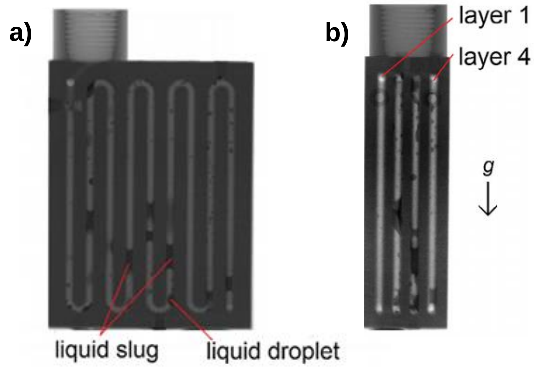

Figure 17. Neutron radiographs of four inter-connected layered heat pipe (50.8 × 38.1 × 15.75 mm^3) with residual water slugs and droplets where: (a) Front and (b) Side view [170]. Reprinted from Int J Heat Mass Transf, 108, Ibrahim et al., An investigation of a multi-layered oscillating heat pipe additively manufactured from Ti-6Al-4V powder, p. 1036-1047, 2017, with permission from Elsevier

Jafari *et al*. [171] manufactured a stainless-steel porous structure for heat pipe with an average pore size of 160 µm. The study focused on the establishment of the effective thermal conductivity of the wick structure under evacuated conditions and when it was filled with ethylene glycol or water.

Due to the development of compact electronic applications, thermal management of the heat generated has become an enormous challenge. Consequently, extensive research efforts have focused on the development of heat sinks that can effectively disperse heat to mitigate hot spots. Advanced manufacturing methods have been critical to overcoming technological challenges for thermal management in high-power modules and packaging systems. Syed-Khaja *et al*. [172] noted that for high power applications, temperatures can reach elevated levels of 200 °C and higher at the interconnected level. As such, the design of the packaging of such a system becomes extremely critical. As a result, a heat sink was developed for high-power electronic systems and demonstrated that a significant reduction in volume, weight, and maximum chip temperatures can be achieved. Li *et al*., [173] used additive manufacturing for the thermal management of batteries where unprecedented area and specific capacity was enabled by extrusion-based additive manufacturing. Similarly, Ferrari *et al*. [174], Fu *et al*. [175] and Sun *et al*. [176] investigated performance improvement by utilizing high-performance thermal management for micro batteries enabled by advanced manufacturing. Another application, where the design of improved heat sinks is critical, are advanced illumination systems. Kim *et al*. [177] and Lin *et al*. [178] reported that the lifetime of the LED-based illumination system is considerably shortened by hot spots. Consequently, they developed a heat pipe and heat sink based solutions using advanced manufacturing processes.

The development of highly efficient fuel cells is critical for clean energy production. Despite the extensive capital cost, there has been an increasing interest in various types of fuel cell technologies due to their higher efficiency and reduced environmental impact. As a result, extensive research has been devoted to the development of thermal management of fuel cells using advanced manufacturing. Kaushik and Bourell [179], used additive manufacturing to fabricate electrically conductive bipolar plates for a direct methanol fuel cell application and demonstrated a significant performance improvement. Similarly, Guo and Leu [180], evaluated the electrical conductivity of bipolar plates produced by additive manufacturing to those produced by injection and compression molding. In another study [181], a bio-inspired "leaf" design was developed for bipolar plates which demonstrated a significant enhancement in the power density of the fuel cell. Figure 18 illustrates some of the designs for bipolar plates used in various studies produced by additive manufacturing.

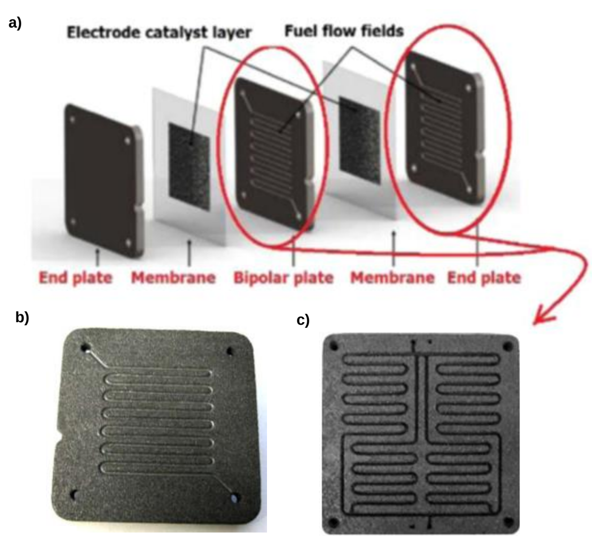

Figure 18. (a) Fuel cell stack (b) midsection of bipolar plate (50 × 50 × 5 mm) [179]. Reprinted from Rapid Prototyp J, 16, Alayavalli and Bourell, Fabrication of modified graphite bipolar plates by indirect selective laser sintering (SLS) for direct methanol fuel cells, 268-74, 2010, with permission from Emerald Insight (c) Serpentine bipolar plate (50 × 50 × 4 mm) [180]. Reprinted from Int J Hydrogen Energy, 37, Effect of different graphite materials on the electrical conductivity and flexural strength of bipolar plates fabricated using selective laser sintering, p. 3558-3566, 2012, with permission from Elsevier

Another relevant area that utilizes advanced manufacturing, is the design of efficient reactors for chemical production. Recent studies in this area have proved that enhancement of two-phase flow for such applications is possible by incorporating high surface area porous media [182]. Hutter *et al*. [182,183], evaluated the performance of tubular reactors deploying commercially available metal foams and free-form porous structure produced by the SLS process. Hutter *et al*. concluded that the fully sintered metallic porous foams provided twice as higher HTC compared to commercially available foams. Figure 19 shows the different porous structures inserted in the tubular reactor.

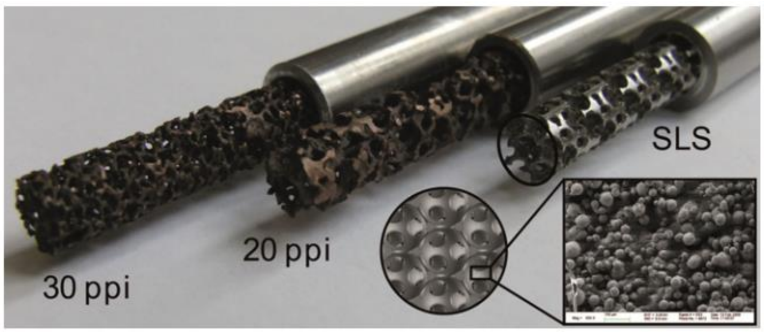

Figure 19. Image of inserted commercial foam elements (20 and 30 ppi) and fully sintered structure (SLS). The SEM image with x500 magnification of SLS indicates the roughness [183] . Reprinted from Chem Eng Sci, 66, Hutter et al., Heat transfer in metal foams and designed porous media, p. 3806-3814, 2011, with permission from Elsevier

While additive manufacturing has been studied in the past, their deployment in commercial applications is often a challenge especially when the equipment cost is a major consideration. However, in some special applications, such as the aerospace industry, the cost is not the decisive factor, and other factors such as the higher specific power and compactness play a more critical role. One of the areas where additive manufacturing has played a crucial role in such an industry is the development of advanced electro-thermal propulsion systems. To achieve a compact solution with high-temperature thermal management for aircrafts, Romei *et al*. [184] utilized the SLS process and achieved highly refined feature sizes using 316 stainless steel (Fig. 20a,b). Saltzman *et al*. [185] and Hathaway *et al*. [186], fabricated an oil cooling system for aerospace applications and reported a major reduction in the weight of the device with a noticeable performance improvement. Vanapalli *et al*. [187] manufactured a highly compact flat-panel gas-gap heat switch (Fig. 20c-g) to provide cooling in cryogenic temperature ranges using helium, hydrogen, and nitrogen as the working fluids.

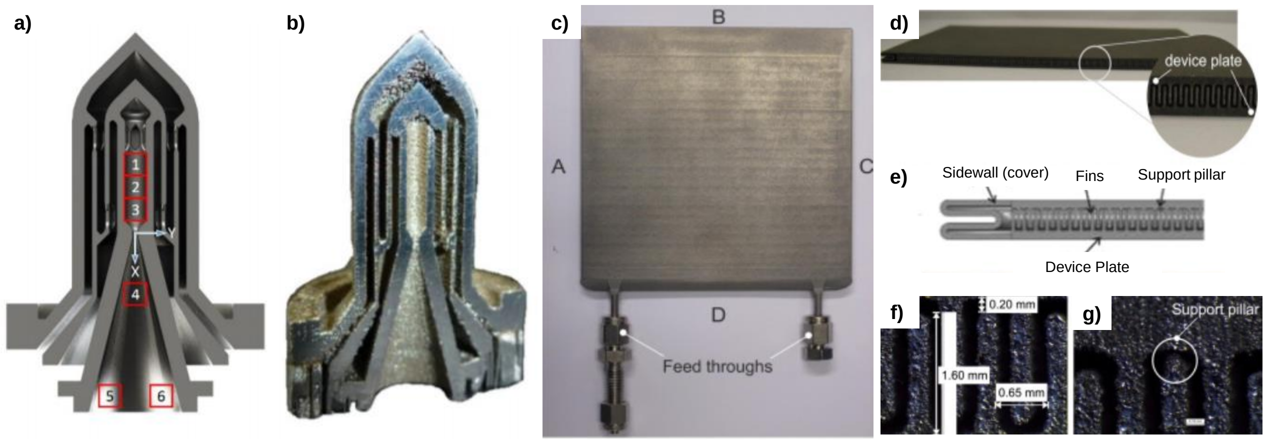

Figure 20. AM manufactured Heat exchanger half-section with 0.42 mm nozzle throat diameter: (a) Schematic and (b) Manufactured part [184]. Reprinted from Acta Astronaut, 138, Romei et al., Manufacturing of a high-temperature resistojet heat exchanger by selective laser melting, 356-68, 2017, with permission from Elsevier. (c) Heat switch of size 11 cm × 11 cm × 3.2 mm (d) Cut section of the heat switch, (e) Fins in contact with device base (f)Image of fin dimensions, and (g) Image of support pillars [187]. Adapted from Cryogenics (Guildf), 78, Vanapalli et al., Cryogenic flat-panel gas-gap heat switch, p. 83-88, 2016, with permission from Elsevier

In conclusion, advanced manufacturing technology has a major impact on enhancing two-phase flow. The development of complex porous structures and embedded systems has opened a new field of ultra-compact and highly efficient solutions. While the majority of the existing literature focused on enhanced pool boiling, the developments in additive manufacturing have also provided opportunities to develop efficient two-phase flow systems such as heat pipes. Furthermore, several application-based solutions have been proposed for highly compact heat sinks, and heat exchangers including high power electronics, fuel cells, and aerospace.

5.0 Discussion:

This work presents a comprehensive review of heat transfer augmentation techniques for two-phase flows required in the design and development of next-generation heat exchangers. Generally, these enhanced heat exchangers can be manufactured by either conventional manufacturing techniques or other advanced manufacturing techniques such as AM. To summarize, Tables 3 and 4 highlight the most important findings in the flow boiling and flow condensation research fields, respectively. Furthermore, Table 5 summarizes efficiency correlations along with proper citations to aid future design. Several different techniques were reviewed, each of which has its strengths and limitations. The first method studied was the deployment of surfactants inside the flowing two-phase fluid. Surfactant additives are not intrusive and would not require any change to the existing designs. Therefore, such a technique is relatively inexpensive to implement. However, the use of surfactants is limited to lower heat fluxes as well as for higher surface tension working fluids such as water or ethylene glycol. As the heat flux increases, the adsorbed surfactant molecules on the tube surface no longer adhere to the surface, allowing the tube to return to its original state [58]. Moreover, surfactant additives may not be appropriate for some industries, such as the food industry, in which surfactant could be considered as a contaminant. Although some surfactants were demonstrated to enhance HTC, others did not [59]. The second set of enhancement techniques include the deployment of inserts, namely coils, or tapes. Using such inserts is a cost-effective way to enhance in-tube heat transfer. Inserts are easy to install and additional treatment to the tubes is not required. However, it is important to keep in mind that such inserts would need to be replaced occasionally, as they are susceptible to wear or fouling[188]. Aside from inserts, other popular techniques such as extended surfaces, dimples, and ribs directly modify the tube wall geometry. Note that such techniques could also be used to augment heat transfer in single-phase flows [189]. Unlike other passive techniques, such as tape and wire coil inserts, dimpled tubes or tubes with ribs incur less maintenance cost as there is no need to replace tapes or inserts. Furthermore, the risk of blockage is minimal. However, implementing such tubing on existing systems is difficult because smooth tubes would need to be replaced with ones with dimples/ribs. Inserts (coils/tapes) may not have this issue. Finally, as shown in Table 2, dimples can cause significant pressure drops. As highlighted previously, extended surfaces can take many different geometries such as fins and herringbone. Micro-fins on tubes offer a solution to achieve heat transfer enhancement. Although it might be relatively more challenging to manufacture fins than to simply add a tape insert, fins provide in many cases much higher heat transfer enhancement than pressure drop increase. However, for evaporative two-phase flows, the added benefit of micro-fins is mainly justifiable for lower mass fluxes. Therefore, if the existing system has a high flow rate, other enhancement techniques should be sought out. Another positive feature that fins provide in condensation applications is self-drainage. Since thin film condensate tends to form on the tip of the fin, the surface tension of the fluid pulls the film in the valley located in between the fins. This not only provides self-drainage, but it also has the added benefit of reducing the liquid film resistance [31]. Although herringbone tubes are similar in concept to micro-fin tubes, the herringbone pattern can provide a higher heat transfer enhancement. However, compared with micro-fin tubes, herringbone tubes result in much larger pressure drops and could be relatively more complex to manufacture. Similar to dimpled tubes, herringbone tubes incur fewer maintenance costs as there is no need to replace tapes or inserts except when the fouling of the tube itself occurs [190]. Finally, the risk of tube blockage is minimal. The last set of enhancement techniques reviewed are active techniques with a focus on EHD. Active techniques, in general, pertain to advantageous characteristics absent in all other passive techniques mentioned above. They can provide a much larger heat transfer augmentation and provide the ability to control the amount of heat transfer enhancement. This ability is granted by varying the output supply to the desired amount.

Active techniques are seldomly adopted in the industry due to how difficult it is to integrate them into pre-existing systems. Unlike passive techniques that just require a tube exchange, having an active technique such as EHD, would require an electric wire to run through the tube with a high potential difference. This may not always be suitable and poses an electric hazard during the operation. Furthermore, EHD only operates on dielectric fluids. This hinders the use of EHD in FMCGs since the fluid in the heat exchangers is the product being manufactured. Therefore, EHD is not suitable in applications where the fluid cannot be exchanged for another. Another point to consider is the cost of operation. Passive techniques such as dimples, require only an initial investment to replace the tubes but do not incur any further costs during operation. However, for active techniques similar to EHD, the need for a constantly running power supply during operation translates into continuous expenses. Further, the precautions needed to ensure the system is electrically insulated incur further expenditures to set up the system.

From the aforementioned discussion, it can be noted that the most suitable technique for heat transfer enhancement is circumstantial. If the most substantial enhancement is sought, EHD would be most suitable, however, it is expensive and difficult to implement. As a consequence, active techniques are usually not adopted as much in the industry. If ease of implementation is the main concern, then changing the fluid behavior by using surfactants would prove to be one of the easiest and cheapest techniques. However, tampering with the liquid is not always permissible especially in FMCGs. A more balanced technique that is widely used in industries due to its aforementioned advantages and acceptable limitations is micro-fins [191]. That being said, the effectiveness of micro-fins is dependent on their shape, inclination, height, and so on. The optimal micro-fin geometry is also circumstantial and is application dependent. However, commercially available vendors exist to facilitate the decision-making process.

The previous discussion was limited to conventional techniques adopted to facilitate heat transfer enhancement. Recent developments, however, shifted towards additive manufacturing (AM) to cause heat transfer enhancement [192]. Utilizing the AM enhancement techniques reviewed in this paper would not only enable more compact heat exchangers, but it also enables the fabrication of micro-heat exchangers that is needed in many electronic device applications [193]. Consequently, AM can overcome the manufacturing limitations of conventional manufacturing techniques. Furthermore, since AM relies on depositing layers one after the other to manufacture components, this enables unprecedented flexibility in manufacturing complex geometries that would have been otherwise very challenging to implement using conventional manufacturing techniques [194]. Furthermore, this added flexibility enables the implementation of heat exchangers that are very customizable and situation specific. Moreover, AM does not require secondary processes such as machining to achieve required geometrical shapes This cuts down production time and the cost of multiple manufacturing equipment [195]. Also, since AM is a layer-by-layer deposition technique, it can save on material because unlike conventional methods such as milling, it does not depend on removing material to achieve the desired geometry [195]. Another advantage AM possesses over other techniques, is its ability to use different materials, such as metals, plastics, or ceramics to manufacture a single part.

Even though AM revolutionized manufacturing and reflects recent advancements in the field, it has challenges that limit its adoption over conventional techniques. First, heat exchangers manufactured using AM are limited in size and must be essentially smaller than the 3D printer.

For large-sized parts, large printers are needed, prompting a high upfront capital investment. Furthermore, surface finishing of AM parts usually needs to be followed up by post processes to obtain the desired tolerance [196,197]. Another challenge with AM processes is scaling [195]. For highly customizable heat exchangers with complex geometries, AM manufacturing is cheaper. However, limitations in production speed mean that for simple geometries AM would not be able to sustain large production rates and benefit from economies of scale that would have been realized otherwise by conventional manufacturing techniques.

Table 3. Summary of flow boiling enhancement techniques.

No.	Passive/Active	Type of enhancement	Author	Fluid	Results*
1	Passive	Surfactant	Qiu *et al.* [58]	Octadecylamine	Increase in heat transfer enhancement
2			Hetsroni *et al.* [60]	Water and water-surfactant (Habon G)	Increase in heat transfer enhancement and pressure drop
3		Dimples	Shafaee *et al.* [61]	R600a	HTC increased by 1.29–2 times. Pressure drop was higher by 7 to 103%
4			Zahid *et al.* [69]	R134a	With rid insert: HTC increased threefold. Pressure drop increased
5			Guo *et al.* [66]	R22, R410A, R32	Heat transfer enhancement increased by up to 1.2–1.4 times
6			Wei *et al.* [71]	R410A	HTC increased by 1.11–1.43 times
7		Micro-fin	Schlager *et al.* [74]	R22	HTC increased by 1.6–2.2 times. Pressure drop increased
8			Yu *et al.* [77]	R134a	Heat transfer enhanced up to 200% at low mass

					flux and higher quality
9			Zhnag *et al.* [75]	R417A	EF amounted to 1.26-2.8 and PF amounted to 1.8-2.6.
10			Schlager *et al.* [82]	R22	Heat transfer enhancement ranging from 50 to 100% The maximum increase in pressure drop was 40%.
11			Oh and Bergles [83]	R134a	Optimal helix angle for maximum HTC depended on mass flux conditions.
12			Kimura and Ito [84]	R12	Spiral-grooved tube can increase HTC from 1.5-2 times for annular flow, and approximately 10 times for stratified flow
13			Yang and Hrnjak [85]	R410A	Annular flow occurred at lower mass flux and vapor qualities as the helix angle increased.

14			Chiang [86]	R22	Heat transfer augmentation in the axial micro-finned tube was larger than the helical micro-fin tube
15			Wu *et al.* [87]	R32	Increase the heat transfer by 60% and pressure drop by 40%
16			Yang and Hrnjak [88]	R410A	Increase the heat transfer by 1.34 times and pressure drop by 1.23 times
17			Jiang *et al.* [76]	R22, R134a, R407C, and R410A	Average HTC of R134a, R22, R410A, and R407C are 1.80, 1.86, 1.78, and 1.69 times higher. Average pressure drop of R134a, R22, R410A, and R407C are 1.30, 1.42, 1.40, and 1.45 times higher, respectively
18			Diani *et al.* [78]	R1234ze(E)	HTC increased by 2.4 times. Pressure drop increased by 1.4 times

19			Filho and Barbieri [79]	R134a	HTC and pressure drop increased
20			Kim and Shin [80]	R22 and R410a	HTC increased 1.64–2.99 and 1.86–3.27 times for R410a and R22, respectively
21			Dang *et al.* [81]	Carbon dioxide	HTC increased by 1.9–2.3 times. Pressure drop increased by 1.5–2.1 times
22		Herringbone tube	Guo *et al.* [66]	R22, R410A, and R32	No improvement
23			Olivier *et al.* [91]	R22, R407C, and R134a	Heat transfer enhancement 70% higher. Pressure drop 80% higher
24			Longo *et al.* [92]	R22	HTC increased by 1.3–1.4 times
25			Filho and Jabardo [93]	R134a	Herringbone has superior thermal performance and pressure drop compared with micro-fin tubes
26		Twisted tape	Sarmadian *et al.* [94]	R600a	HTC and pressure drop increased. The PFE values ranged between 0.44-1.09

27			Kanizawa *et al.* [95]	R134a	HTC improved to a maximum of 45%. Pressure drop increased by a maximum of 30 times
28			Shishkin *et al.* [96]	R134a	Tapes induced an annular flow regime earlier. Mass and heat fluxes higher than 400 kg/m²s and 100 kW/m², respectively did not affect HTC.
29			Yan *et al.* [97]	Water	Increased CHF significantly under high mass fluxes
30		Wired coil	Behabadi *et al.* [98]	R134a	HTC improved to a maximum of 98%. Pressure drop increased by a maximum of 1000%
31			Niezgoda-Żelasko [100]	R507, R410, and R407C	HTC for azeotropic fluids increased by 1.1-1.7 times, while the HTC for zeotropic agents increased by 1.1-1.3 times. Pressure

					drop increased by 1.8-4.5 times
32			Alimardani *et al.* [101]	R600a	Pressure drop increased by 90-958%. The PFE values ranged between 0.13-1.4
33			Yun *et al.*[102]	Nitrogen	HTC and pressure drop increased, with PFE values >1
34	Active	EHD	Cotton *et al.* [113]	HFC-134a	Average HTC increased threefold in annular channels while pressure drop increased 2.6 times
35			Cotton *et al.* [114]	HFC-134a	Heat transfer was enhanced 1.6 times while the pressure drop increased 1.2 times
36			Salehi *et al.* [115]	R134a	Boiling HTC increased tenfold at 3 kV
37			Liu *et al.* [116]	R123	Maximum enhancement factor amounted to 20.1 for an average electric field strength of

					1333 kV/m in vertical tubes

**Compared with smooth tubes with no modifications unless stated otherwise.*

Table 4. Summary of condensation heat transfer enhancement techniques.

No.	Passive/Active	Type of enhancement	Author	Fluid	Results*
1	Passive	Twisted tape	Hejazi *et al.* [125]	HFC-134a	Increase in HTC of 40% in best cases. Pressure drop increase of 2.4 times in worst cases
2			Akhavan-Behabadi *et al.* [126]	R134a	Heat transfer coefficients increase up to 38% at low mass fluxes
3			Agrawal *et al.* [127]	R22	Increased heat transfer by up to 25% for full-length twisted tape insert
4		Wired coil	Agrawal *et al.* [128]	R22	HTC increase of up to 100%
5			Akhavan-Behabadi *et al.* [131]	R134a	Pressure drop increase of 260–1600%
6			Salimpour and Gholami [132]	R404A	Pressure drop increase of 1300%
7		Corrugated tube	Laohalertdecha and Wongwises [133]	R134a	HTC increase of up to 50%. Frictional pressure drop increase of up to 70%
8			Khoeini *et al.* [134]	R134a	HTC increase of 1.27–1.41 times at an inclination of 30° compared with an inclination of −90°
9			Fernández-Seara and Uhía [135]	NH_3	Heat transfer performance of corrugated tubes on the outside was 1.27 times higher
10		Microfin tube	Jung *et al.* [136]	R22, R134a, R407C, and R410A	HTC increase of twofold to threefold
11			Kwon *et al.* [137]	R22 and R410A	Enhancement ratio between 1.5 - 2.2 based on the nominal heat transfer area

12			Eckels and Pate [138]	R134a and CFC-12	For HFC-134a, HTC increase of 1.75–2.5 times. For CFC-12, HTC increases of 1.7–2.3 times. Pressure drop increase
13			Naulboonrueng *et al.* [139]	HFC-134a	HTC increase of 1.1–1.85 times.
14			Naulboonrueng and Wongwises [140]	HFC-134a	Pressure drop increase of 10–50%
15			Eckels *et al.* [142]	R134a with ester lubricant	Heat transfer increase of 50–200%. Pressure drop increase of 10–50%
16			Cho and Tae [143]	R22 and R407C with oil	Before bend: Oil concentrations decreased heat transfer augmentation At bend: Maximum HTC After bend: Higher HTC than before bend
17			Graham *et al.* [141]	R135a	For mass fluxes around 150 kg/m^2s, axially grooved tubes provide better thermal performance than helically grooved or smooth tubes. Pressure drop for axially grooved tube and helically grooved tube are similar and both are higher than for smooth tubes
18		Herringbone groove tube	Miyara *et al.* [144]	R410A and R22	Thermal performance is superior to that of helical microfin tubes at high velocities and vice versa for low velocities. Pressure drop of herringbone tube is greater than that of microfin tube
19			Miyara *et al.* [145]	R410A	Longer fins increase heat transfer up to a height of 0.18 mm.

					HTC increases with helical angle. Pressure drop increase with height and helix angle
20			Goto *et al*. [146]	R410A and HCFC22	Herringbone groove provides twice the increase in HTC compared with the spiraled groove
21			Goto *et al*. [147]	R410A and R22	Herringbone groove provides twice the increase in HTC compared with the spiraled groove
22	Active	EHD	Gidwani *et al*. [148]	R134a, R407c and R404a	For R404a at 18 kV: Heat transfer was enhanced 18.8 times for smooth tubes and 5.8 times for corrugated tubes. Pressure drop increased 11.8 times for smooth tubes. For R134a at 18 kV: Heat transfer increased 8.3 times for corrugated tubes. Pressure drop increased 20.8 times for corrugated tubes. For R407c at 18 kV: Heat transfer enhancement increased 3.9 times for smooth tubes and 2.9 times for corrugated tubes
23			Choi [149]	Freon-113	HTC increase of 100% at 30 kV downstream in vertical tubes
24			Didkovsky and Bologa [150]	Water	Heat transfer increase of 20 times compared with tubes with no EHD in vertical tubes

**Compared with smooth tubes with no modifications unless stated otherwise.*

Table 5. Efficiency correlations for flow boiling.

Authors	Correlation	Nomenclature
Shafee *et al.* [61]	$PFS = \frac{h_a}{h_\mathrm{p}} . \frac{A_\mathrm{p}}{A_a}$	h_a: average heat transfer coefficient in augmented tubes h_p: average heat transfer coefficient in plain tubes A_p: total inner surface area of the plain tube A_a: total inner surface area of the augmented tubes
	$PFE = \frac{(\frac{h_\mathrm{a}}{h_\mathrm{p}})}{(\frac{\Delta P_\mathrm{a}}{\Delta P_\mathrm{p}})}$	h_a: average heat transfer coefficient in augmented tubes h_p: average heat transfer coefficient in plain tubes ΔP_a: Pressure drop in augmented tubes ΔP_p: Pressure drop in the plain tube
Promvonge [198]	$\mathrm{PEC} = \left(\frac{\mathrm{Nu_a}}{\mathrm{Nu_0}}\right)\left(\frac{f_\mathrm{a}}{f_0}\right)^{-1/3}$	η: Thermal Performance factor $\mathrm{Nu_a}$: Nusselt number augmented $\mathrm{Nu_0}$: Nusselt number smooth f_a: Friction factor augmented f_a: Friction factor smooth
Schlager *et al.* [74]	$EF = \frac{(hA)_{Enhanced\ tube}}{(hA)_{Smooth\ tube}}$	h: average heat transfer coefficient A: total inner surface area
	$PF = \frac{(\Delta P)_{Enhanced\ tube}}{(\Delta P)_{Smooth\ tube}}$	ΔP: Change in pressure

A dire need to begin to implement the reviewed enhancements in next-generation heat exchangers exists. Global energy consumption has steadily grown throughout the past century (Fig. 21) [199]. With 63% of the global generated thermal energy being lost across different temperature spectrums [200] as waste heat during heat transfer and conversion processes [201], it becomes essential to develop highly efficient systems that can capture the majority of the consumed energy resources. Since the majority of heat transfer processes utilizes a heat exchanger, an effort is needed to maximize their efficiency. The main approach to elevating the heat exchanger efficiency is through enhancing the HTC. Having a higher HTC increases the maximum heat flux that can be transmitted and reduces energy lost during conversion [202]. Moreover, being able to transfer a larger amount of heat per unit area allows for more efficient heat exchange and so longer tubes can be substituted for smaller ones while achieving the same goal. Since more compact heat exchangers are enabled through the proposed techniques, the ability to decrease material consumption, which is projected to further increase as shown in Fig. 22, is facilitated. Decreased material consumption in turn aids in the development of more sustainable systems and industries.

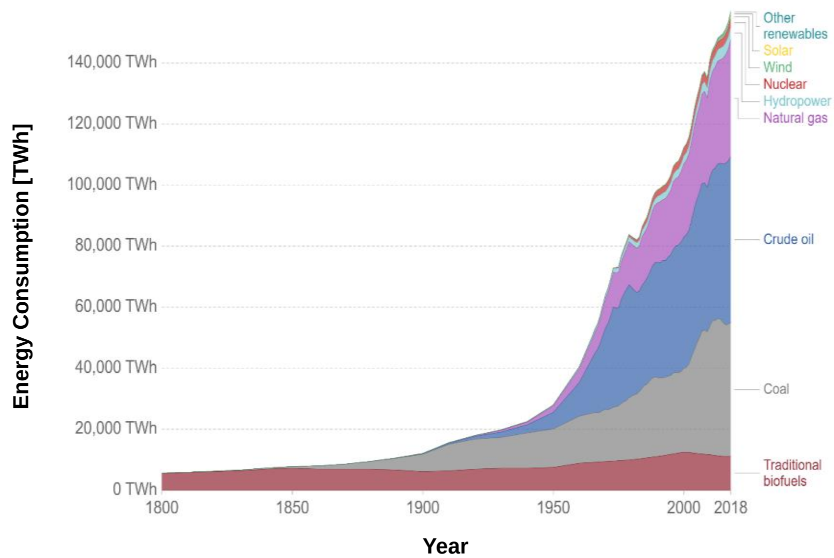

Figure 21. Global energy consumption from the year 1800 to 2018 [199]. Adapted with permission from Hannah Ritchie (2014) - "Energy". Published online at OurWorldInData.org. Retrieved from: 'https://ourworldindata.org/energy'.

While it is relatively easy to develop new systems with the appropriate enhancement techniques, the greatest concern of adopting two-phase flow enhancement techniques is the ease of integration for already existing heat exchangers which cannot be retrofitted. As noted in the previous discussions and Tables 3 and 4, a wide array of cost-effective solutions exist which do not require major overhaul or disruption to already established processes. For example, dimples and twisted tapes can be implemented with minimal integration penalty when compared to other enhancements such as micro-fin tubes. The cost of the equipment required for integrating such enhancements is also another major challenge. A typical heat exchanger manufacturer would require major economic benefits before the infrastructure can be acquired to replace conventional technology. Consequently, compliance is always a major concern. For example, for tube and fin heat exchangers, replacing plain tubes with micro-fin tubes will require appropriate expansion technology which does not damage the fins during an expansion (pneumatic vs. bullet and rod expansion). Furthermore, durability and maintenance requirements are critical. For example, plain tubes have less potential for fouling compared to internally enhanced tubes.

Advanced manufacturing approaches such as additive manufacturing can bring remarkable performance improvements by invoking solutions that are not possible with conventional manufacturing approaches at both the design and material levels. However, for such processes, evaluation of materials is mandatory to meet specific thermal and mechanical properties. The manufacturing process has a major impact on these parameters and as such can influence the design of the device. For such processes, the design, material selection, and manufacturing are highly interrelated and unlike conventional approaches, an additional cost is associated with such interrelation. Nonetheless, with the continued growth of greenhouse gas emissions worldwide [203] and the expansion of heavy industries to meet the demand of developing nations, building new heat exchangers is inevitable. Consequently, it is worthwhile to ensure that new thermal systems are being built with maximal efficiency by taking into consideration all the available enhancement techniques. This would not only aid in providing economic growth for industries but also aid in the responsible consumption of resources and mitigation of global warming for future generations.

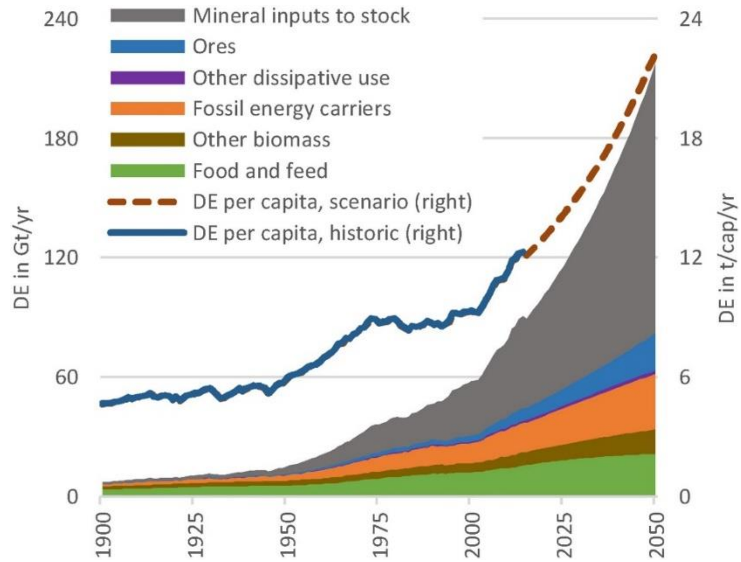

Figure 22. Extraction of materials (DE) in the US from the years 1900 to 2050 (projected) [204]. Reprinted from Glob Environ Chang, 52, Krausmann et al., From resource extraction to outflows of wastes and emissions: The socioeconomic metabolism of the global economy, 1900–2015., 131-40, 2018, with permission from Elsevier

6.0 Conclusions

This paper reviews existing and emerging passive and active techniques to augment two-phase heat transfer. Passive techniques such as tapes, fins, and dimples are covered, demonstrating their benefit in enhancing heat transfer. Further, the use of electric fields (EHD) to augment heat transfer is discussed. Although EHD can be somewhat more involved in terms of cost and safety considerations, it provides the most capacity to increase the HTC. The EHD technique also provides control over the heat transfer by controlling the applied voltage and extent of HTC enhancement. However, whether active or passive enhancement is considered, a common trait for all techniques is the resulting additional pressure drop and consequent pumping power. Therefore, it is important that the savings from the use of smaller heat exchangers, enabled by enhancements, outweigh the added costs incurred from having to use a larger pump and more energy to operate the system. To capture this trade-off, several enhancement factors are presented to compare techniques. The value of these factors depends on the extent of the enhancement in heat transfer which, in turn, depends on several parameters. For example, for passive techniques such as coil inserts, the diameter, feature pitch ratio, and mass flux govern the heat transfer augmentation. For active techniques such as EHD, the position of the electric wire and the polarity impacts the rate of heat transfer. Furthermore, the flow regime and the fluid affect the heat transfer enhancement. For example, the use of surfactants to change the surface tension of the liquid facilitates evaporation. Although many techniques are reviewed for both condensation and boiling/evaporating flows, this work is not exhaustive, as the field continually develops.

Acknowledgments:

This research was supported in part by an appointment to the Oak Ridge National Laboratory ASTRO Program, sponsored by the U.S. Department of Energy and administered by the Oak Ridge Institute for Science and Education. N.M. and M. M. gratefully acknowledge funding support by the National Science Foundation Engineering Research Center for Power Optimization of Electro Thermal Systems (POETS) with cooperative agreement EEC-1449548. N.M. gratefully acknowledges funding support from the International Institute for Carbon Neutral Energy Research (WPI-I2CNER), sponsored by the Japanese Ministry of Education, Culture, Sports, Science, and Technology. All figures appearing in this paper were obtained with approved permission from Ren21, OurWorldinData, Elsevier, and Emerald (through RightsLink).

References:

[1] Mousa MH, Günay AA, Orejon D, Khodakarami S, Nawaz K, Miljkovic N. Gas-Phase Temperature Mapping of Evaporating Microdroplets. ACS Appl Mater Interfaces 2021;13:15925–38. https://doi.org/10.1021/acsami.1c02790.

[2] Mousa MH, Miljkovic N, Nawaz K. Review of heat transfer enhancement techniques for single phase flows. Renew Sustain Energy Rev 2021;137:110566. https://doi.org/10.1016/j.rser.2020.110566.

[3] Nations U. Special edition: progress towards the Sustainable Development Goals. 2019.

[4] Boyina KS, Mahvi AJ, Chavan S, Park D, Kumar K, Lira M, et al. Condensation frosting on meter-scale superhydrophobic and superhydrophilic heat exchangers. Int J Heat Mass Transf 2019;145:118694. https://doi.org/10.1016/j.ijheatmasstransfer.2019.118694.

[5] Energy Efficiency Trends in Residential and Commercial Buildings. n.d.

[6] Agonafer D, Spector MS, Miljkovic N. Materials and Interface Challenges in High Vapor Quality Two-Phase Flow Boiling Research. IEEE Trans Components, Packag Manuf Technol 2021:1–1. https://doi.org/10.1109/TCPMT.2021.3085255.

[7] Habibi Khalaj A, Halgamuge SK. A Review on efficient thermal management of air- and liquid-cooled data centers: From chip to the cooling system. Appl Energy 2017;205:1165–88. https://doi.org/10.1016/j.apenergy.2017.08.037.

[8] R. K, L. M. Conceptualizing green IT and data center power and cooling issues 2007.

[9] Renewables 2019 Global Status Report. REN21 2019.

[10] Orubu CO. Using Transportation Control Measures and Economic Instruments to Reduce Air Pollution Due to Automobile Emissions. J Soc Sci 2004;8:227–36. https://doi.org/10.1080/09718923.2004.11892419.

[11] Chou D, Liao Z, Fernandez K, Gebrael T, Popovic G, Mahony R, et al. An Interleaved 6-Level GaN Bidirectional Converter with an Active Energy Buffer for Level II Electric Vehicle Charging. 2021 IEEE Appl. Power Electron. Conf. Expo., IEEE; 2021, p. 1203–8. https://doi.org/10.1109/APEC42165.2021.9487122.

[12] Zhang T, Gao C, Gao Q, Wang G, Liu M, Guo Y, et al. Status and development of electric vehicle integrated thermal management from BTM to HVAC. Appl Therm Eng 2015;88:398–409. https://doi.org/10.1016/j.applthermaleng.2015.02.001.

[13] Cvok I, Škugor B, Deur J. Control trajectory optimisation and optimal control of an electric vehicle HVAC system for favourable efficiency and thermal comfort. Optim Eng 2020. https://doi.org/10.1007/s11081-020-09515-w.

[14] Yang T, King WP, Miljkovic N. Phase change material-based thermal energy storage. Cell Reports Phys Sci 2021;2:100540. https://doi.org/10.1016/j.xcrp.2021.100540.

[15] Yang T, Braun P V., Miljkovic N, King WP. Phase Change Material Heat Sink for Transient Cooling of High-Power Devices. Int J Heat Mass Transf 2021;170:121033. https://doi.org/10.1016/j.ijheatmasstransfer.2021.121033.

[16] Yang T, Kang JG, Weisensee PB, Kwon B, Braun P V., Miljkovic N, et al. A composite phase change material thermal buffer based on porous metal foam and low-melting-temperature metal alloy. Appl Phys Lett 2020;116:071901. https://doi.org/10.1063/1.5135568.

[17] Taylor P, Bergles AE, V JHL, Kendall GE, Griffith P. Boiling and Evaporation in Small Diameter Channels Small Diameter Channels 2013;24:37–41. https://doi.org/10.1080/01457630390116086.

[18] Thome JR. Boiling in microchannels: a review of experiment and theory. Int J Heat Fluid Flow 2004;25:128–39. https://doi.org/10.1016/j.ijheatfluidflow.2003.11.005.

[19] Ni G, Miljkovic N, Ghasemi H, Huang X, Boriskina S V., Lin C-T, et al. Volumetric solar heating of nanofluids for direct vapor generation. Nano Energy 2015;17:290–301. https://doi.org/10.1016/j.nanoen.2015.08.021.

[20] Moon H, Miljkovic N, King WP. High power density thermal energy storage using additively manufactured heat exchangers and phase change material. Int J Heat Mass Transf 2020;153:119591. https://doi.org/10.1016/j.ijheatmasstransfer.2020.119591.

[21] Birbarah P, Gebrael T, Foulkes T, Stillwell A, Moore A, Pilawa-Podgurski R, et al. Water immersion cooling of high power density electronics. Int J Heat Mass Transf

2020;147:118918. https://doi.org/10.1016/j.ijheatmasstransfer.2019.118918.

[22] Sett S, Sokalski P, Boyina K, Li L, Rabbi KF, Auby H, et al. Stable Dropwise Condensation of Ethanol and Hexane on Rationally Designed Ultrascalable Nanostructured Lubricant-Infused Surfaces. Nano Lett 2019;19:5287–96. https://doi.org/10.1021/acs.nanolett.9b01754.

[23] Li L, Lin Y, Rabbi KF, Ma J, Chen Z, Patel A, et al. Fabrication Optimization of Ultra-Scalable Nanostructured Aluminum-Alloy Surfaces. ACS Appl Mater Interfaces 2021;13:43489–504. https://doi.org/10.1021/acsami.1c08051.

[24] Ma J, Porath LE, Haque MF, Sett S, Rabbi KF, Nam S, et al. Ultra-thin self-healing vitrimer coatings for durable hydrophobicity. Nat Commun 2021;12:5210. https://doi.org/10.1038/s41467-021-25508-4.

[25] Ma J, Sett S, Cha H, Yan X, Miljkovic N. Recent developments, challenges, and pathways to stable dropwise condensation: A perspective. Appl Phys Lett 2020;116:260501. https://doi.org/10.1063/5.0011642.

[26] Oh J, Hoffman JB, Hong S, Jo KD, Román-Kustas J, Reed JH, et al. Dissolvable Template Nanoimprint Lithography: A Facile and Versatile Nanoscale Replication Technique. Nano Lett 2020;20:6989–97. https://doi.org/10.1021/acs.nanolett.0c01547.

[27] Sheikholeslami M, Abohamzeh E, Jafaryar M, Shafee A, Babazadeh H. CuO nanomaterial two-phase simulation within a tube with enhanced turbulator. Powder Technol 2020;373:1–13. https://doi.org/10.1016/j.powtec.2020.06.017.

[28] He W, Toghraie D, Lotfipour A, Pourfattah F, Karimipour A, Afrand M. Effect of twisted-tape inserts and nanofluid on flow field and heat transfer characteristics in a tube. Int Commun Heat Mass Transf 2020;110:104440. https://doi.org/10.1016/j.icheatmasstransfer.2019.104440.

[29] Eiamsa-ard S, Wongcharee K, Eiamsa-ard P, Thianpong C. Heat transfer enhancement in a tube using delta-winglet twisted tape inserts. Appl Therm Eng 2010;30:310–8. https://doi.org/10.1016/j.applthermaleng.2009.09.006.

[30] Mohammadi A, Koşar A. Review on Heat and Fluid Flow in Micro Pin Fin Heat Sinks

under Single-phase and Two-phase Flow Conditions. Nanoscale Microscale Thermophys Eng 2018;22:153–97. https://doi.org/10.1080/15567265.2018.1475525.

[31] Bejan A, Kraus AD. Heat Transfer Handbook. 2003.

[32] Zohuri B. Application of Compact Heat Exchangers For Combined Cycle Driven Efficiency In Next Generation Nuclear Power Plants. 1st editio. Springer; 2016.

[33] Suh Y, Lee J, Simadiris P, Yan X, Sett S, Li L, et al. A Deep Learning Perspective on Dropwise Condensation. Adv Sci 2021:2101794. https://doi.org/10.1002/advs.202101794.

[34] Hobold GM, da Silva AK. Machine learning classification of boiling regimes with low speed, direct and indirect visualization. Int J Heat Mass Transf 2018;125:1296–309. https://doi.org/10.1016/j.ijheatmasstransfer.2018.04.156.

[35] Niknam SA, Mortazavi M, Li D. Additively manufactured heat exchangers: a review on opportunities and challenges. Int J Adv Manuf Technol 2021;112:601–18. https://doi.org/10.1007/s00170-020-06372-w.

[36] Mills AF. Heat and Mass Transfer. Routledge; 2018. https://doi.org/10.4324/9780203752173.

[37] Lienhard IV JH, Lienhard V JH. A Heat Transfer Textbook. 5.10. 2020.

[38] Carey VP. Liquid-vapor phase-change phenomena. 1st ed. Hemisphere; 1992.

[39] Akhavan-Behabadi MA, Salimpour MR, Pazouki VA. Pressure drop increase of forced convective condensation inside horizontal coiled wire inserted tubes. Int Commun Heat Mass Transf 2008;35:1220–6. https://doi.org/10.1016/j.icheatmasstransfer.2008.06.004.

[40] Steiner D. VDI-Wärmeatlas (VDI heat atlas). Verein Dtsch Ingenieure, VDI-Gesellschaft Verfahrenstechnik Und Chemieingenieurwes (GCV), Düsseld 1993.

[41] Gnielinski V. New equations for heat and mass transfer in turbulent pipe and channel flow. Int Chem Eng 1976;16:359–68.

[42] Petukhov BS. Heat transfer and friction in turbulent pipe flow with variable physical properties. Adv Heat Transf 1970;6:i565.

[43] Fernández-Seara J, Uhía FJ, Sieres J, Campo A. A general review of the Wilson plot method and its modifications to determine convection coefficients in heat exchange devices. Appl Therm Eng 2007;27:2745–57. https://doi.org/10.1016/j.applthermaleng.2007.04.004.

[44] Wilson EE. A basis for rational design of heat transfer apparatus. J Am Soc Mech Engrs 1915;37:546–51.

[45] Li J, Zhu G, Kang D, Fu W, Zhao Y, Miljkovic N. Endoscopic Visualization of Contact Line Dynamics during Pool Boiling on Capillary-Activated Copper Microchannels. Adv Funct Mater 2021;31:2006249. https://doi.org/10.1002/adfm.202006249.

[46] Bowers MB, Mudawar I. Two-Phase Electronic Cooling Using Mini-Channel and Micro-Channel Heat Sinks: Part 2—Flow Rate and Pressure Drop Constraints. J Electron Packag 1994;116:298. https://doi.org/10.1115/1.2905701.

[47] Bowers MB, Mudawar I. Two-Phase Electronic Cooling Using Mini-Channel and Micro-Channel Heat Sinks: Part 1—Design Criteria and Heat Diffusion Constraints. J Electron Packag 1994;116:290. https://doi.org/10.1115/1.2905700.

[48] Lian Zhang, Jae-Mo Koo, Linan Jiang, Asheghi M, Goodson KE, Santiago JG, et al. Measurements and modeling of two-phase flow in microchannels with nearly constant heat flux boundary conditions. J Microelectromechanical Syst 2002;11:12–9. https://doi.org/10.1109/84.982858.

[49] Li J, Kang D, Fazle Rabbi K, Fu W, Yan X, Fang X, et al. Liquid film–induced critical heat flux enhancement on structured surfaces. Sci Adv 2021;7:eabg4537. https://doi.org/10.1126/sciadv.abg4537.

[50] Zhu Y, Antao DS, Chu K-H, Chen S, Hendricks TJ, Zhang T, et al. Surface Structure Enhanced Microchannel Flow Boiling. J Heat Transfer 2016;138. https://doi.org/10.1115/1.4033497.

[51] Upot NV, Mahvi A, Fazle Rabbi K, Li J, Jacobi AM, Miljkovic N. Scalable and Resilient Etched Metallic Micro- and Nanostructured Surfaces for Enhanced Flow Boiling. ACS Appl Nano Mater 2021;4:6648–58. https://doi.org/10.1021/acsanm.1c00524.

[52] Ma J, Cha H, Kim M, Cahill DG, Miljkovic N. Condensation Induced Delamination of Nanoscale Hydrophobic Films. Adv Funct Mater 2019;29:1905222. https://doi.org/10.1002/adfm.201905222.

[53] Yang YM, Maa JR. Pool Boiling of Dilute Surfactant Solutions. J Heat Transfer 1983;105:190. https://doi.org/10.1115/1.3245541.

[54] Tzan YL, Yang YM. Experimental Study of Surfactant Effects on Pool Boiling Heat Transfer. J Heat Transfer 1990;112:207. https://doi.org/10.1115/1.2910346.

[55] Yu Min Yang. Dynamic surface effect on boiling of aqueous surfactant solutions. Int Commun Heat Mass Transf 1990;17:711–27. https://doi.org/10.1016/0735-1933(90)90018-F.

[56] Wu W-T, Yang Y-M, Maa J-R. Enhancement of Nucleate Boiling Heat Transfer and Depression of Surface Tension by Surfactant Additives. J Heat Transfer 1995;117:526. https://doi.org/10.1115/1.2822558.

[57] Wu W-T, Yang Y-M, Maa J-R. Technical Note Pool boiling incipience and vapor bubble growth dynamics in surfactant solutions. Int J Heat Mass Transf 1999;42:2483–8. https://doi.org/10.1016/S0017-9310(98)00335-4.

[58] Qiu Y, Chen W, Si Q. Enhancement of flow boiling heat transfer with surfactant. J Cent South Univ Technol 2007;7:219–22. https://doi.org/10.1007/s11771-000-0058-0.

[59] Cheng L, Mewes D, Luke A. Boiling phenomena with surfactants and polymeric additives: A state-of-the-art review. Int J Heat Mass Transf 2007;50:2744–71. https://doi.org/10.1016/j.ijheatmasstransfer.2006.11.016.

[60] Hetsroni G, Gurevich M, Mosyak A, Rozenblit R. Drag reduction and heat transfer of surfactants flowing in a capillary tube. Int J Heat Mass Transf 2004;47:3797–809. https://doi.org/10.1016/j.ijheatmasstransfer.2004.03.009.

[61] Shafaee M, Mashouf H, Sarmadian A, Mohseni SG. Evaporation heat transfer and pressure drop characteristics of R-600a in horizontal smooth and helically dimpled tubes. Appl Therm Eng 2016;107:28–36. https://doi.org/10.1016/j.applthermaleng.2016.06.148.

[62] Kurylo MJ. The chemistry of stratospheric ozone: its response to natural and anthropogenic influences. Int J Refrig 1990;13:62–72. https://doi.org/10.1016/0140-7007(90)90003-F.

[63] Molina MJ, Rowland FS. Stratospheric sink for chlorofluoromethanes: Chlorine atomc-atalysed destruction of ozone. Nature 1974. https://doi.org/10.1038/249810a0.

[64] Hibiki T, Ishii M. Thermo-fluid Dynamics of Two-Phase Flow. 2nd ed. Springer Science & Business Media; 2010.

[65] Ghiaasiaan SM. Two-Phase Flow, Boiling, and Condensation: In Conventional and Miniature Systems. Cambridge University Press; 2007.

[66] Guo SP, Wu Z, Li W, Kukulka D, Sundén B, Zhou XP, et al. Condensation and evaporation heat transfer characteristics in horizontal smooth, herringbone and enhanced surface EHT tubes. Int J Heat Mass Transf 2015;85:281–91. https://doi.org/10.1016/j.ijheatmasstransfer.2015.01.115.

[67] Agrawal K., Varma H. Experimental study of heat transfer augmentation versus pumping power in a horizontal R12 evaporator. Int J Refrig 1991;14:273–81. https://doi.org/10.1016/0140-7007(91)90042-F.

[68] Li M, Khan TS, Al Hajri E, Ayub ZH. Geometric optimization for thermal–hydraulic performance of dimpled enhanced tubes for single phase flow. Appl Therm Eng 2016;103:639–50. https://doi.org/10.1016/j.applthermaleng.2016.04.141.

[69] Ayub ZH, Ayub AH, Ribatski G, Moreira TA, Khan TS. Two-phase pressure drop and flow boiling heat transfer in an enhanced dimpled tube with a solid round rod insert. Int J Refrig 2017;75:1–13. https://doi.org/10.1016/j.ijrefrig.2017.01.008.

[70] Tibiriçá CB, Ribatski G. Flow patterns and bubble departure fundamental characteristics during flow boiling in microscale channels. Exp Therm Fluid Sci 2014;59:152–65. https://doi.org/10.1016/j.expthermflusci.2014.02.017.

[71] Li W, Chen J, Zhu H, Kukulka DJ, Minkowycz WJ. Experimental study on condensation and evaporation flow inside horizontal three dimensional enhanced tubes. Int Commun Heat Mass Transf 2017;80:30–40.

https://doi.org/10.1016/j.icheatmasstransfer.2016.11.006.

[72] Fujie K, Itoh M, Innami T, Kimura H, Nakayama W, Yanugidi T. US patent No. 4044797 A, 1977.

[73] Newell TA, Shah RK. An Assessment of Refrigerant Heat Transfer, Pressure Drop, and Void Fraction Effects In Microfin Tubes. HVAC&R Res 2001;7:125–53. https://doi.org/10.1080/10789669.2001.10391267.

[74] Schlager LM, Pate MB, Bergles AE. Evaporation and Condensation Heat Transfer and Pressure Drop in Horizontal, 12.7-mm Microfin Tubes With Refrigerant 22. J Heat Transfer 1990;112:1041. https://doi.org/10.1115/1.2910476.

[75] Zhang X, Zhang J, Ji H, Zhao D. Heat transfer enhancement and pressure drop performance for R417A flow boiling in internally grooved tubes. Energy 2015;86:446–54. https://doi.org/10.1016/j.energy.2015.04.054.

[76] Jiang GB, Tan JT, Nian QX, Tang SC, Tao WQ. Experimental study of boiling heat transfer in smooth/micro-fin tubes of four refrigerants. Int J Heat Mass Transf 2016;98:631–42. https://doi.org/10.1016/j.ijheatmasstransfer.2016.03.024.

[77] Yu M, Lin T, Tseng C. Heat transfer and flow pattern during two-phase flow boiling of R-134a in horizontal smooth and microfin tubes. Int J Refrig 2002;25:789–98. https://doi.org/10.1016/S0140-7007(01)00075-5.

[78] Diani A, Mancin S, Cavallini A, Rossetto L. Experimental investigation of R1234ze(E) flow boiling inside a 2.4 mm ID horizontal microfin tube. Int J Refrig 2016;69:272–84. https://doi.org/10.1016/j.ijrefrig.2016.06.014.

[79] Bandarra Filho EP, Barbieri PEL. Flow boiling performance in horizontal microfinned copper tubes with the same geometric characteristics. Exp Therm Fluid Sci 2011;35:832–40. https://doi.org/10.1016/j.expthermflusci.2010.06.012.

[80] Kim M-H, Shin J-S. Evaporating heat transfer of R22 and R410A in horizontal smooth and microfin tubes. Int J Refrig 2005;28:940–8. https://doi.org/10.1016/j.ijrefrig.2005.01.016.

[81] Dang C, Haraguchi N, Hihara E. Flow boiling heat transfer of carbon dioxide inside a small-sized microfin tube. Int J Refrig 2010;33:655–63. https://doi.org/10.1016/j.ijrefrig.2010.01.003.

[82] Schlager L., Pate M., Bergles A. Heat transfer and pressure drop during evaporation and condensation of R22 in horizontal micro-fin tubes. Int J Refrig 1989;12:6–14. https://doi.org/10.1016/0140-7007(89)90006-6.

[83] Oh S-Y, Bergles AE. Microfin Tube Technology — the Effects of Spiral Angle on Evaporative Heat Transfer Enhancement. Heat Transf. Enhanc. Heat Exch., Dordrecht: Springer Netherlands; 1999, p. 67–78. https://doi.org/10.1007/978-94-015-9159-1_5.

[84] H K, M I. Evaporating Heat Transfer in Horizontal Internal Spiral-grooved Tubes in the Region of Low Flow Rates. JSME Int J 1981;24:1602–7.

[85] Yang C-M, Hrnjak P. Effect of helical micro-fins on two-phase flow behavior of R410A evaporating in horizontal round tubes obtained through visualization. Int J Heat Mass Transf 2019;144:118654. https://doi.org/10.1016/j.ijheatmasstransfer.2019.118654.

[86] Chiang R. Heat transfer and pressure drop during evaporation and condensation of refrigerant-22 in 7.5 mm and 10mm diameter axial and helical grooved tubes. AIChE J 1993;89:205–10.

[87] Wu X, Zhu Y, Huang X. Influence of 0° helix angle micro fins on flow and heat transfer of R32 evaporating in a horizontal mini multichannel flat tube. Exp Therm Fluid Sci 2015;68:669–80. https://doi.org/10.1016/j.expthermflusci.2015.07.010.

[88] Yang C-M, Hrnjak P. Effect of straight micro fins on heat transfer and pressure drop of R410A during evaporation in round tubes. Int J Heat Mass Transf 2018;117:924–39. https://doi.org/10.1016/j.ijheatmasstransfer.2017.10.064.

[89] Yang C-M, Hrnjak P. Visualization of two-phase flow of R410A in horizontal smooth and axial micro-finned tubes. Int J Heat Mass Transf 2019;138:49–58. https://doi.org/10.1016/j.ijheatmasstransfer.2019.03.174.

[90] Wellsandt S, Vamling L. Prediction method for flow boiling heat transfer in a herringbone microfin tube. Int J Refrig 2005;28:912–20. https://doi.org/10.1016/j.ijrefrig.2005.01.009.

[91] Olivier JA, Liebenberg L, Thome JR, Meyer JP. Heat transfer, pressure drop, and flow pattern recognition during condensation inside smooth, helical micro-fin, and herringbone tubes. Int J Refrig 2007;30:609–23. https://doi.org/10.1016/j.ijrefrig.2006.11.003.

[92] Longo G., Gasparella A, Sartori R. Experimental heat transfer coefficients during refrigerant vaporisation and condensation inside herringbone-type plate heat exchangers with enhanced surfaces. Int J Heat Mass Transf 2004;47:4125–36. https://doi.org/10.1016/j.ijheatmasstransfer.2004.05.001.

[93] Bandarra Filho EP, Saiz Jabardo JM. Convective boiling performance of refrigerant R-134a in herringbone and microfin copper tubes. Int J Refrig 2006;29:81–91. https://doi.org/10.1016/j.ijrefrig.2005.05.011.

[94] Sarmadian A, Moghaddam HA, Asnaashari A, Joushani HAN, Moosavi M, Islam MS, et al. Flow boiling heat transfer and pressure drop characteristics of Isobutane in horizontal channels with twisted tapes. Int J Heat Mass Transf 2020;162:120345. https://doi.org/10.1016/j.ijheatmasstransfer.2020.120345.

[95] Kanizawa FT, Mogaji TS, Ribatski G. Evaluation of the heat transfer enhancement and pressure drop penalty during flow boiling inside tubes containing twisted tape insert. Appl Therm Eng 2014;70:328–40. https://doi.org/10.1016/j.applthermaleng.2014.05.029.

[96] Shishkin A, Kanizawa FT, Ribatski G, Tarasevich S, Yakovlev A. Experimental investigation of the heat transfer coefficient during convective boiling of R134a in tubes with twisted tape insert. Int J Refrig 2018;92:196–207. https://doi.org/10.1016/j.ijrefrig.2018.06.002.

[97] Yan J, Bi Q, Zhu G, Cai L, Yuan Q, Lv H. Critical heat flux of highly subcooled water flow boiling in circular tubes with and without internal twisted tapes under high mass fluxes. Int J Heat Mass Transf 2016;95:606–19. https://doi.org/10.1016/j.ijheatmasstransfer.2015.12.024.

[98] Akhavan-Behabadi MA, Mohseni SG, Najafi H, Ramazanzadeh H. Heat transfer and pressure drop characteristics of forced convective evaporation in horizontal tubes with coiled wire inserts. Int Commun Heat Mass Transf 2009;36:1089–95.

https://doi.org/10.1016/j.icheatmasstransfer.2009.07.009.

[99] Varma HK, Agrawal KN, Bansal M. Turbulence promoters in horizontal R22 evaporators. AIRAH 1992;46:21–30.

[100] Niezgoda-Żelasko B. Heat Transfer and Pressure Drop Measurements During Boiling in Vertical Tubes with Coiled-Wire Inserts. Heat Transf Eng 2019;40:1633–48. https://doi.org/10.1080/01457632.2018.1480880.

[101] Alimardani F, Moghaddam HA, Sarmadian A, Shafaee M. Pressure loss and performance assessment of horizontal spiral coil inserted pipes during forced convective evaporation of R-600a. Int J Refrig 2019;107:20–30. https://doi.org/10.1016/j.ijrefrig.2019.08.016.

[102] Yun R, Hwang J-S, Chung JT, Kim Y. Flow boiling heat transfer characteristics of nitrogen in plain and wire coil inserted tubes. Int J Heat Mass Transf 2007;50:2339–45. https://doi.org/10.1016/j.ijheatmasstransfer.2006.10.038.

[103] Allen PHG, Karayiannis TG. Electrohydrodynamic enhancement of heat transfer and fluid flow. Heat Recover Syst CHP 1995;15:389–423. https://doi.org/10.1016/0890-4332(95)90050-0.

[104] KARAYIANNIS TG, COLLINS MW, ALLEN PHG. ELECTROHYDRODYNAMIC ENHANCEMENT OF NUCLEATE BOILING HEAT TRANSFER IN HEAT EXCHANGERS. Chem Eng Commun 1989;81:15–24. https://doi.org/10.1080/00986448908940528.

[105] Jalaluddin AK, Sinha DB. Effect of an electric field on the superheat of liquids. Nuovo Cim 1962;26:234–7. https://doi.org/10.1007/BF02824277.

[106] Eames IW, Sabir HM. Potential benefits of electrohydrodynamic enhancement of two-phase heat transfer in the design of refrigeration systems. Appl Therm Eng 1997;17:79–92. https://doi.org/10.1016/1359-4311(96)00012-9.

[107] Laohalertdecha S, Naphon P, Wongwises S. A review of electrohydrodynamic enhancement of heat transfer. Renew Sustain Energy Rev 2007;11:858–76. https://doi.org/10.1016/j.rser.2005.07.002.

[108] Markels M, Durfee RL. The effect of applied voltage on boiling heat transfer. AIChE J 1964;10:106–10. https://doi.org/10.1002/aic.690100130.

[109] Ogata J, Yabe A. Augmentation of boiling heat transfer by utilizing the EHD effect—EHD behaviour of boiling bubbles and heat transfer characteristics. Int J Heat Mass Transf 1993;36:783–91. https://doi.org/10.1016/0017-9310(93)80054-X.

[110] Damianidis C, Karayiannis TG, Al-Dadah A, James RW, Collins MW, Allen PHG. EHD boiling enhancement in shell-and-tube evaporators and its application in refrigeration plants. ASHRAE Trans., vol. 98, 1992, p. 462–72.

[111] Yan YY, Karayiannis TG, Allen PHG, Neve R. EHD enhancement of boiling heat transfer at low superheat surfaces in heat exchangers. Recent Dev. Heat Exch. Technol., Paris: 1993.

[112] P. cooper. Electrically enhanced heat transfer in the shell/tube heat exchanger. University of London, 1986.

[113] Cotton JS, Robinson AJ, Shoukri M, Chang JS. AC voltage induced electrohydrodynamic two-phase convective boiling heat transfer in horizontal annular channels. Exp Therm Fluid Sci 2012;41:31–42. https://doi.org/10.1016/j.expthermflusci.2012.03.003.

[114] Cotton JS, Chang JS, Shoukri M, Smith-Pollard T. Electrohydrodynamically enhanced flow boiling in an eccentric horizontal cylindrical channel. Annu. Rep. Conf. Electr. Insul. Dielectr. Phenom., IEEE; n.d., p. 220–3. https://doi.org/10.1109/CEIDP.2002.1048775.

[115] Salehi M, Ohadi MM, Dessiatoun S. EHD Enhanced Convective Boiling of R-134a in Grooved Channels—Application to Subcompact Heat Exchangers. J Heat Transfer 1997;119:805. https://doi.org/10.1115/1.2824186.

[116] Liu Y, Li R, Wang F, Yu H. The effect of electrode polarity on EHD enhancement of boiling heat transfer in a vertical tube. Exp Therm Fluid Sci 2005;29:601–8. https://doi.org/10.1016/j.expthermflusci.2004.07.004.

[117] Weisensee PB, Wang Y, Qian H, Schultz D, King WP, Miljkovic N. Condensate droplet size distribution on lubricant-infused surfaces. Int J Heat Mass Transf 2017;109:187–99. https://doi.org/10.1016/j.ijheatmasstransfer.2017.01.119.

[118] Enright R, Miljkovic N, Alvarado JL, Kim K, Rose JW. Dropwise Condensation on Micro- and Nanostructured Surfaces. Nanoscale Microscale Thermophys Eng 2014;18:223–50. https://doi.org/10.1080/15567265.2013.862889.

[119] Miljkovic N, Wang EN. Condensation heat transfer on superhydrophobic surfaces. MRS Bull 2013;38:397–406. https://doi.org/10.1557/mrs.2013.103.

[120] Cho HJ, Preston DJ, Zhu Y, Wang EN. Nanoengineered materials for liquid–vapour phase-change heat transfer. Nat Rev Mater 2017;2:16092. https://doi.org/10.1038/natrevmats.2016.92.

[121] Miljkovic N, Enright R, Wang EN. Effect of Droplet Morphology on Growth Dynamics and Heat Transfer during Condensation on Superhydrophobic Nanostructured Surfaces. ACS Nano 2012;6:1776–85. https://doi.org/10.1021/nn205052a.

[122] Shahriari A, Birbarah P, Oh J, Miljkovic N, Bahadur V. Electric Field–Based Control and Enhancement of Boiling and Condensation. Nanoscale Microscale Thermophys Eng 2017;21:102–21. https://doi.org/10.1080/15567265.2016.1253630.

[123] Manglik RM. Heat transfer enhancement of intube flows in process heat exchangers by means of twisted-tape inserts. Rensselaer Polytechnic Institute, 1991.

[124] Kreith F, Margolis D. Heat transfer and friction in turbulent vortex flow. Appl Sci Res 1959;8:457–73. https://doi.org/10.1007/BF00411769.

[125] Hejazi V, Akhavan-Behabadi MA, Afshari A. Experimental investigation of twisted tape inserts performance on condensation heat transfer enhancement and pressure drop. Int Commun Heat Mass Transf 2010;37:1376–87. https://doi.org/10.1016/j.icheatmasstransfer.2010.07.021.

[126] Akhavan-Behabadi MA, Kumar R, Rajabi-najar A. Augmentation of heat transfer by twisted tape inserts during condensation of R-134a inside a horizontal tube. Heat Mass Transf 2008;44:651–7. https://doi.org/10.1007/s00231-007-0297-9.

[127] Agrawal KN, Kumar R, Lal SN, Varma HK. Heat Transfer Augmentation by Segmented Tape Inserts During Condensation of R-22 Inside a Horizontal Tube. ASHRAE Trans 2004;110:143–50.

[128] Agrawal KN, Kumar A, Akhavan Behabadi MA, Varma HK. Heat transfer augmentation by coiled wire inserts during forced convection condensation of R-22 inside horizontal tubes. Int J Multiph Flow 1998;24:635–50. https://doi.org/10.1016/S0301-9322(97)00061-X.

[129] Said SA, Azer NZ. Heat transfer and pressure drop during condensation inside horizontal tubes with twisted tape inserts. ASHRAE Trans 1983;89:96–113.

[130] Said SA, Azer NZ. Heat transfer and pressure drop during condensation inside horizontal finned tubes. ASHRAE Trans 1983;89:114–34.

[131] Akhavan-Behabadi MA, Salimpour MR, Pazouki VA. Pressure drop increase of forced convective condensation inside horizontal coiled wire inserted tubes. Int Commun Heat Mass Transf 2008;35:1220–6. https://doi.org/10.1016/j.icheatmasstransfer.2008.06.004.

[132] Salimpour MR, Gholami H. Effect of inserting coiled wires on pressure drop of R-404A condensation. Int J Refrig 2014;40:24–30. https://doi.org/10.1016/j.ijrefrig.2013.10.013.

[133] Laohalertdecha S, Wongwises S. The effects of corrugation pitch on the condensation heat transfer coefficient and pressure drop of R-134a inside horizontal corrugated tube. Int J Heat Mass Transf 2010;53:2924–31. https://doi.org/10.1016/j.ijheatmasstransfer.2010.01.037.

[134] Khoeini D, Akhavan-Behabadi MA, Saboonchi A. Experimental study of condensation heat transfer of R-134a flow in corrugated tubes with different inclinations. Int Commun Heat Mass Transf 2012;39:138–43. https://doi.org/10.1016/j.icheatmasstransfer.2011.09.011.

[135] Fernández-Seara J, Uhía FJ. Heat transfer and friction characteristics of spirally corrugated tubes for outer ammonia condensation. Int J Refrig 2012;35:2022–32. https://doi.org/10.1016/j.ijrefrig.2012.05.021.

[136] Jung D, Cho Y, Park K. Flow condensation heat transfer coefficients of R22, R134a, R407C, and R410A inside plain and microfin tubes. Int J Refrig 2004;27:25–32. https://doi.org/10.1016/S0140-7007(03)00122-1.

[137] Kwon J-T, Park SK, Kim MH. Enhanced Effect of a Horizontal Micro-fin Tube for

Condensation Heat Transfer with R22 and R410A. J Enhanc Heat Transf 2000;7:97–107. https://doi.org/10.1615/JEnhHeatTransf.v7.i2.30.

[138] Eckels SJ, Pate MB. EVAPORATION AND CONDENSATION OF HFC-134a AND CFC-12 IN A SMOOTH TUBE AND A MICRO-FIN TUBE. ASHRAE Trans 1389;97:68–78.

[139] Naulboonrueng T, Kaewon J, Wongwises S. Two-phase condensation heat transfer coefficients of HFC –134a at high mass flux in smooth and micro-fin tubes. Int Commun Heat Mass Transf 2003;30:577–90. https://doi.org/10.1016/S0735-1933(03)00086-1.

[140] Nualboonrueng T, Wongwises S. TWO-PHASE FLOW PRESSURE DROP OF HFC-134a DURING CONDENSATION IN SMOOTH AND MICRO-FIN TUBES AT HIGH MASS FLUX. Int Commun Heat Mass Transf 2004;31:991–1004. https://doi.org/10.1016/j.icheatmasstransfer.2004.05.009.

[141] Graham D, Chato JC, Newell T a. Heat transfer and pressure drop during condensation of refrigerant 134a in an axially grooved tube. Int J Heat Mass Transf 1999;42:1935–44. https://doi.org/10.1016/S0017-9310(98)00307-X.

[142] Eckels SJ, Doerr TM, Pate MB. Heat transfer coefficients and pressure drops for R-134a and an ester lubricant mixture in a smooth tube and a micro-fin tube. ASHRAE Trans., 1998.

[143] Cho K, Tae S-J. Condensation heat transfer for R-22 and R-407C refrigerant–oil mixtures in a microfin tube with a U-bend. Int J Heat Mass Transf 2001;44:2043–51. https://doi.org/10.1016/S0017-9310(00)00253-2.

[144] Miyara A, Nonaka K, Taniguchi M. Condensation heat transfer and flow pattern inside a herringbone-type micro-fin tube. Int J Refrig 2000;23:141–52. https://doi.org/10.1016/S0140-7007(99)00037-7.

[145] Miyara A, Otsubo Y, Ohtsuka S, Mizuta Y. Effects of fin shape on condensation in herringbone microfin tubes. Int J Refrig 2003;26:417–24. https://doi.org/10.1016/S0140-7007(02)00154-8.

[146] Goto M, Inoue N, Ishiwatari N. Condensation and evaporation heat transfer of R410A

inside internally grooved horizontal tubes. Int J Refrig 2001;24:628–38. https://doi.org/10.1016/S0140-7007(00)00087-6.

[147] Goto M, Inoue N, Yonemoto R. Condensation heat transfer of R410A inside internally grooved horizontal tubes. Int J Refrig 2003;26:410–6. https://doi.org/10.1016/S0140-7007(02)00153-6.

[148] Gidwani A, Molki M, Ohadi MM. EHD-Enhanced Condensation of Alternative Refrigerants in Smooth and Corrugated Tubes. HVAC&R Res 2002;8:219–37. https://doi.org/10.1080/10789669.2002.10391439.

[149] Choi HY. Electrohydrodynamic Condensation Heat Transfer. J Heat Transfer 1968;90:98. https://doi.org/10.1115/1.3597468.

[150] Didkovsky AB, Bologa MK. Vapour film condensation heat transfer and hydrodynamics under the influence of an electric field. Int J Heat Mass Transf 1981;24:811–9. https://doi.org/10.1016/S0017-9310(81)80004-X.

[151] Kwon B, Foulkes T, Yang T, Miljkovic N, King WP. Air Jet Impingement Cooling of Electronic Devices Using Additively Manufactured Nozzles. IEEE Trans Components, Packag Manuf Technol 2020;10:220–9. https://doi.org/10.1109/TCPMT.2019.2936852.

[152] Moon H, Boyina K, Miljkovic N, King WP. Heat Transfer Enhancement of Single-Phase Internal Flows using Shape Optimization and Additively Manufactured Flow Structures. Int J Heat Mass Transf 2021;177:121510. https://doi.org/10.1016/j.ijheatmasstransfer.2021.121510.

[153] Ho JY, Liu P, Leong KC, Wong TN, Miljkovic N. A theoretical analysis and parametric study of filmwise condensation on three-dimensional pin fins. Int J Heat Mass Transf 2021;171:121092. https://doi.org/10.1016/j.ijheatmasstransfer.2021.121092.

[154] Egbo M, Nasersharifi Y, Hwang G. Phase-change heat transfer of sintered-particle wick in downward facing orientation: Particle size and wick thickness effects. Int J Heat Mass Transf 2020;155:119840. https://doi.org/10.1016/j.ijheatmasstransfer.2020.119840.

[155] Patil CM, Kandlikar SG. Review of the Manufacturing Techniques for Porous Surfaces Used in Enhanced Pool Boiling. Heat Transf Eng 2014;35:887–902.

https://doi.org/10.1080/01457632.2014.862141.

[156] Li J, Fu W, Zhang B, Zhu G, Miljkovic N. Ultrascalable Three-Tier Hierarchical Nanoengineered Surfaces for Optimized Boiling. ACS Nano 2019;13:14080–93. https://doi.org/10.1021/acsnano.9b06501.

[157] Ho JY, Wong KK, Leong KC. Saturated pool boiling of FC-72 from enhanced surfaces produced by Selective Laser Melting. Int J Heat Mass Transf 2016;99:107–21. https://doi.org/10.1016/j.ijheatmasstransfer.2016.03.073.

[158] Wong KK, Leong KC. Saturated pool boiling enhancement using porous lattice structures produced by Selective Laser Melting. Int J Heat Mass Transf 2018;121:46–63. https://doi.org/10.1016/j.ijheatmasstransfer.2017.12.148.

[159] Rainey KN, You SM. Pool Boiling Heat Transfer From Plain and Microporous, Square Pin-Finned Surfaces in Saturated FC-72. J Heat Transfer 2000;122:509–16. https://doi.org/10.1115/1.1288708.

[160] Kim TY, Weibel JA, Garimella S V. A free-particles-based technique for boiling heat transfer enhancement in a wetting liquid. Int J Heat Mass Transf 2014;71:808–17. https://doi.org/10.1016/j.ijheatmasstransfer.2013.12.070.

[161] Hoque MJ, Günay A, Stillwell A, Gurumukhi Y, Pilawa-Podgurski RCN, Miljkovic N. Modular Heat Sinks for Enhanced Thermal Management of Electronics. J Electron Packag 2021;143. https://doi.org/10.1115/1.4049294.

[162] Min DH, Hwang GS, Usta Y, Cora ON, Koc M, Kaviany M. 2-D and 3-D modulated porous coatings for enhanced pool boiling. Int J Heat Mass Transf 2009;52:2607–13. https://doi.org/10.1016/j.ijheatmasstransfer.2008.12.018.

[163] Ji X, Xu J, Zhao Z, Yang W. Pool boiling heat transfer on uniform and non-uniform porous coating surfaces. Exp Therm Fluid Sci 2013;48:198–212. https://doi.org/10.1016/j.expthermflusci.2013.03.002.

[164] Deng D, Tang Y, Huang G, Lu L, Yuan D. Characterization of capillary performance of composite wicks for two-phase heat transfer devices. Int J Heat Mass Transf 2013;56:283–93. https://doi.org/10.1016/j.ijheatmasstransfer.2012.09.002.

[165] Jiang L, Ling J, Jiang L, Tang Y, Li Y, Zhou W, et al. Thermal performance of a novel porous crack composite wick heat pipe. Energy Convers Manag 2014;81:10–8. https://doi.org/10.1016/j.enconman.2014.01.044.

[166] Li Y, He J, He H, Yan Y, Zeng Z, Li B. Investigation of ultra-thin flattened heat pipes with sintered wick structure. Appl Therm Eng 2015;86:106–18. https://doi.org/10.1016/j.applthermaleng.2015.04.027.

[167] Ameli M, Agnew B, Leung PS, Ng B, Sutcliffe CJ, Singh J, et al. A novel method for manufacturing sintered aluminium heat pipes (SAHP). Appl Therm Eng 2013;52:498–504. https://doi.org/10.1016/j.applthermaleng.2012.12.011.

[168] Esarte J, Blanco JM, Bernardini A, San-José JT. Optimizing the design of a two-phase cooling system loop heat pipe: Wick manufacturing with the 3D selective laser melting printing technique and prototype testing. Appl Therm Eng 2017;111:407–19. https://doi.org/10.1016/j.applthermaleng.2016.09.123.

[169] Thompson SM, Aspin ZS, Shamsaei N, Elwany A, Bian L. Additive manufacturing of heat exchangers: A case study on a multi-layered Ti–6Al–4V oscillating heat pipe. Addit Manuf 2015;8:163–74. https://doi.org/10.1016/j.addma.2015.09.003.

[170] Ibrahim OT, Monroe JG, Thompson SM, Shamsaei N, Bilheux H, Elwany A, et al. An investigation of a multi-layered oscillating heat pipe additively manufactured from Ti-6Al-4V powder. Int J Heat Mass Transf 2017;108:1036–47. https://doi.org/10.1016/j.ijheatmasstransfer.2016.12.063.

[171] Jafari D, Wits WW, Geurts BJ. An investigation of porous structure characteristics of heat pipes made by additive manufacturing. 2017 23rd Int. Work. Therm. Investig. ICs Syst., IEEE; 2017, p. 1–7. https://doi.org/10.1109/THERMINIC.2017.8233841.

[172] Syed-Khaja A, Freire AP, Kaestle C, Franke J. Feasibility Investigations on Selective Laser Melting for the Development of Microchannel Cooling in Power Electronics. 2017 IEEE 67th Electron. Components Technol. Conf., IEEE; 2017, p. 1491–6. https://doi.org/10.1109/ECTC.2017.232.

[173] Li J, Leu MC, Panat R, Park J. A hybrid three-dimensionally structured electrode for

lithium-ion batteries via 3D printing. Mater Des 2017;119:417–24. https://doi.org/10.1016/j.matdes.2017.01.088.

[174] Ferrari S, Loveridge M, Beattie SD, Jahn M, Dashwood RJ, Bhagat R. Latest advances in the manufacturing of 3D rechargeable lithium microbatteries. J Power Sources 2015;286:25–46. https://doi.org/10.1016/j.jpowsour.2015.03.133.

[175] Fu K, Wang Y, Yan C, Yao Y, Chen Y, Dai J, et al. Graphene Oxide-Based Electrode Inks for 3D-Printed Lithium-Ion Batteries. Adv Mater 2016;28:2587–94. https://doi.org/10.1002/adma.201505391.

[176] Sun K, Wei T-S, Ahn BY, Seo JY, Dillon SJ, Lewis JA. 3D Printing of Interdigitated Li-Ion Microbattery Architectures. Adv Mater 2013;25:4539–43. https://doi.org/10.1002/adma.201301036.

[177] Kim L, Choi JH, Jang SH, Shin MW. Thermal analysis of LED array system with heat pipe. Thermochim Acta 2007;455:21–5. https://doi.org/10.1016/j.tca.2006.11.031.

[178] Lin Z, Wang S, Huo J, Hu Y, Chen J, Zhang W, et al. Heat transfer characteristics and LED heat sink application of aluminum plate oscillating heat pipes. Appl Therm Eng 2011;31:2221–9. https://doi.org/10.1016/j.applthermaleng.2011.03.003.

[179] Alayavalli K, Bourell DL. Fabrication of modified graphite bipolar plates by indirect selective laser sintering (SLS) for direct methanol fuel cells. Rapid Prototyp J 2010;16:268–74. https://doi.org/10.1108/13552541011049289.

[180] Guo N, Leu MC. Effect of different graphite materials on the electrical conductivity and flexural strength of bipolar plates fabricated using selective laser sintering. Proceeding Solid Free Fabr Symp 2012. https://doi.org/10.1016/j.ijhydene.2011.11.058.

[181] Guo N, Leu MC. Experimental study of polymer electrolyte membrane fuel cells using a graphite composite bipolar plate fabricated by selective laser sintering. Proceeding Solid Free Fabr Symp 2012.

[182] Hutter C, Zenklusen A, Lang R, Rudolf von Rohr P. Axial dispersion in metal foams and streamwise-periodic porous media. Chem Eng Sci 2011;66:1132–41. https://doi.org/10.1016/j.ces.2010.12.016.

[183] Hutter C, Büchi D, Zuber V, Rudolf von Rohr P. Heat transfer in metal foams and designed porous media. Chem Eng Sci 2011;66:3806–14. https://doi.org/10.1016/j.ces.2011.05.005.

[184] Romei F, Grubišić AN, Gibbon D. Manufacturing of a high-temperature resistojet heat exchanger by selective laser melting. Acta Astronaut 2017;138:356–68. https://doi.org/10.1016/j.actaastro.2017.05.020.

[185] Saltzman DJ, Bichnevicius M, Lynch SP, Simpson T, Reutzel T, Dickman C, et al. Experimental comparison of a traditionally built versus additively manufactured aircraft heat exchanger. 55th AIAA Aerosp. Sci. Meet., Reston, Virginia: American Institute of Aeronautics and Astronautics; 2017. https://doi.org/10.2514/6.2017-0902.

[186] Hathaway BJ, Garde K, Mantell SC, Davidson JH. Design and characterization of an additive manufactured hydraulic oil cooler. Int J Heat Mass Transf 2018;117:188–200. https://doi.org/10.1016/j.ijheatmasstransfer.2017.10.013.

[187] Vanapalli S, Keijzer R, Buitelaar P, ter Brake HJM. Cryogenic flat-panel gas-gap heat switch. Cryogenics (Guildf) 2016;78:83–8. https://doi.org/10.1016/j.cryogenics.2016.07.006.

[188] Zhao H, Khodakarami S, Deshpande CA, Ma J, Wu Q, Sett S, et al. Scalable Slippery Omniphobic Covalently Attached Liquid Coatings for Flow Fouling Reduction. ACS Appl Mater Interfaces 2021:acsami.1c08845. https://doi.org/10.1021/acsami.1c08845.

[189] Suresh S, Chandrasekar M, Chandra Sekhar S. Experimental studies on heat transfer and friction factor characteristics of CuO/water nanofluid under turbulent flow in a helically dimpled tube. Exp Therm Fluid Sci 2011;35:542–9. https://doi.org/10.1016/j.expthermflusci.2010.12.008.

[190] Zhao H, Khodakarami S, Deshpande CA, Ma J, Wu Q, Sett S, et al. Scalable Slippery Omniphobic Covalently Attached Liquid Coatings for Flow Fouling Reduction. ACS Appl Mater Interfaces 2021;13:38666–79. https://doi.org/10.1021/acsami.1c08845.

[191] Ralph L. Webb, Nae-Hyun Kim. Principles of enhanced heat transfer. 2nd ed. Taylor & Francis.; 2005.

[192] Moon H, McGregor DJ, Miljkovic N, King WP. Coupling of Genetic Algorithm Design with Additive Manufacturing Enables Ultra-Power-Dense Heat Exchanger Development. Joule 2021.

[193] Dede EM, Joshi SN, Zhou F. Topology Optimization, Additive Layer Manufacturing, and Experimental Testing of an Air-Cooled Heat Sink. J Mech Des 2015;137. https://doi.org/10.1115/1.4030989.

[194] Niknam SA, Mortazavi M, Li D. Additively manufactured heat exchangers: a review on opportunities and challenges. Int J Adv Manuf Technol 2020. https://doi.org/10.1007/s00170-020-06372-w.

[195] Bandyopadhyay A, Bose S. Additive Manufacturing. 2nd ed. CRC Press; 2019.

[196] Strano G, Hao L, Everson RM, Evans KE. Surface roughness analysis, modelling and prediction in selective laser melting. J Mater Process Technol 2013;213:589–97. https://doi.org/10.1016/j.jmatprotec.2012.11.011.

[197] Dupuis P, Cormier Y, Fenech M, Corbeil A, Jodoin B. Flow structure identification and analysis in fin arrays produced by cold spray additive manufacturing. Int J Heat Mass Transf 2016;93:301–13. https://doi.org/10.1016/j.ijheatmasstransfer.2015.10.019.

[198] Promvonge P. Thermal augmentation in circular tube with twisted tape and wire coil turbulators. Energy Convers Manag 2008;49:2949–55. https://doi.org/10.1016/j.enconman.2008.06.022.

[199] Ritchie H, Roser M. Energy. Our World Data 2014.

[200] Enova. Potensial for energieffektivisering i norsk landbasert industri. n.d.

[201] Cullen JM, Allwood JM. Theoretical efficiency limits for energy conversion devices. Energy 2010;35:2059–69. https://doi.org/10.1016/j.energy.2010.01.024.

[202] Forman C, Muritala IK, Pardemann R, Meyer B. Estimating the global waste heat potential. Renew Sustain Energy Rev 2016;57:1568–79. https://doi.org/10.1016/j.rser.2015.12.192.

[203] Data.worldbank.org. GDP (constant 2010 US$) | Data 2020.

[204] Krausmann F, Lauk C, Haas W, Wiedenhofer D. From resource extraction to outflows of wastes and emissions: The socioeconomic metabolism of the global economy, 1900–2015. Glob Environ Chang 2018;52:131–40. https://doi.org/10.1016/j.gloenvcha.2018.07.003.